ACS APPLIED POLYMER MATERIALS

pubs.acs.org/acsapm

Review

4D-Printed Shape Memory Polymer Composites: Innovations in Smart Structures, Processing Strategies, and Application Prospects

Xixian Yu, Linlin Wang,* Fenghua Zhang,* and Jinsong Leng

Cite This: *ACS Appl. Polym. Mater.* 2025, 7, 14015−14032

Read Online

ACCESS | Metrics & More | Article Recommendations | Supporting Information

ABSTRACT: Over the past decade, four-dimensional (4D) printing has emerged as a prominent fabrication technique, garnering significant attention. Unlike conventional manufacturing methods, 4D printing enables the transition of materials from static to dynamic configurations. The essence of this technology lies in the integration of smart materials with 3D printing techniques, enabling printed structures to undergo modification of properties under external stimuli. This paper elaborates on 4D printing technologies, including fused deposition modeling (FDM), selective laser sintering (SLS), direct ink writing (DIW), and vat photopolymerization (VP). Furthermore, it provides a comprehensive analysis of diverse shape memory polymers categorized by their actuation mechanisms and examines both current and prospective applications of 4D printing in aerospace, biomedicine, robotics, and electronic devices. These advancements underscore their transformative potential in redefining conventional manufacturing and provide novel solutions to complex engineering challenges. In addition, this review addresses the prevailing challenges in 4D printing technology, including material performance optimization, high-precision/high-efficiency printing, and the need for novel design methodologies. These discussions aim to accelerate the advancement of this burgeoning field.

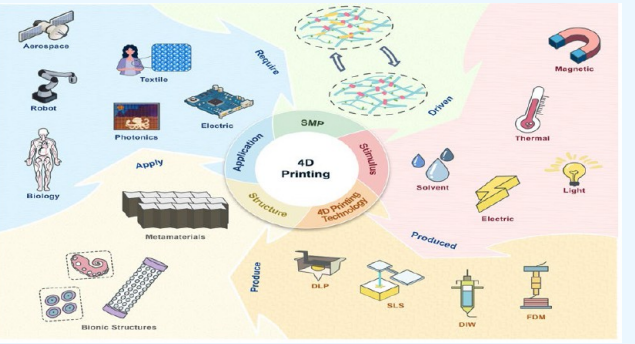

KEYWORDS: *4D printing technology, shape memory polymers, composite materials, smart structures*

1. INTRODUCTION

Three-dimensional (3D) printing technology, also known as additive manufacturing, has evolved into a transformative fabrication method in recent decades,[1] with widespread adoption in aerospace,[2] biomedicine,[3] robotics,[4] and electronics.[5] In contrast to traditional subtractive manufacturing—which removes material from a bulk workpiece (e.g., via lathe machining) to achieve the desired geometries—additive manufacturing constructs objects by sequentially depositing material layers based on computer-aided design (CAD) models. Conventional 3D printing techniques include fused deposition modeling (FDM),[6] selective laser sintering (SLS),[7] direct ink writing (DIW),[8−10] and vat photopolymerization (VP).[11] Recent technological advancements have significantly enhanced the capabilities of multimaterial printing[12] and other sophisticated fabrication strategies. Compared with conventional manufacturing, 3D printing exhibits distinct advantages in fabricating complex geometries while enabling cost-effective small-batch and customized production.[13] Notably, its implementation in product development can reduce associated costs by up to 70% and accelerate time-to-market by approximately 90%, demonstrating the transformative potential for industrial innovation.[14]

At the 2013 TED Conference, Skylar Tibbits[15] from the Massachusetts Institute of Technology (MIT) unveiled a groundbreaking demonstration of 4D printing technology using a rope-like structure that autonomously folded into the letters "MIT" when immersed in water, signifying the advent of a new technological paradigm. Adding the element of time as the fourth dimension to conventional 3D printing (which is based on the X, Y, and Z axes), 4D printing allows printed objects to change their structure, form, and function over time when they come into contact with external stimuli.[16] These stimuli can include things like temperature,[17] light,[18] electric fields,[19] magnetic fields,[20] or solvents.[21] This temporal functionality has placed 4D printing at the forefront of interdisciplinary research. The foundation of this time-dependent shape evolution lies in smart materials—defined as advanced materials capable of perceiving and responding to environmental stimuli (e.g., heat, light, electromagnetic fields,

Received: July 30, 2025
Revised: October 13, 2025
Accepted: October 15, 2025
Published: October 22, 2025

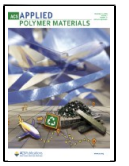

https://doi.org/10.1021/acsapm.5c02816
ACS Appl. Polym. Mater. 2025, 7, 14015−14032

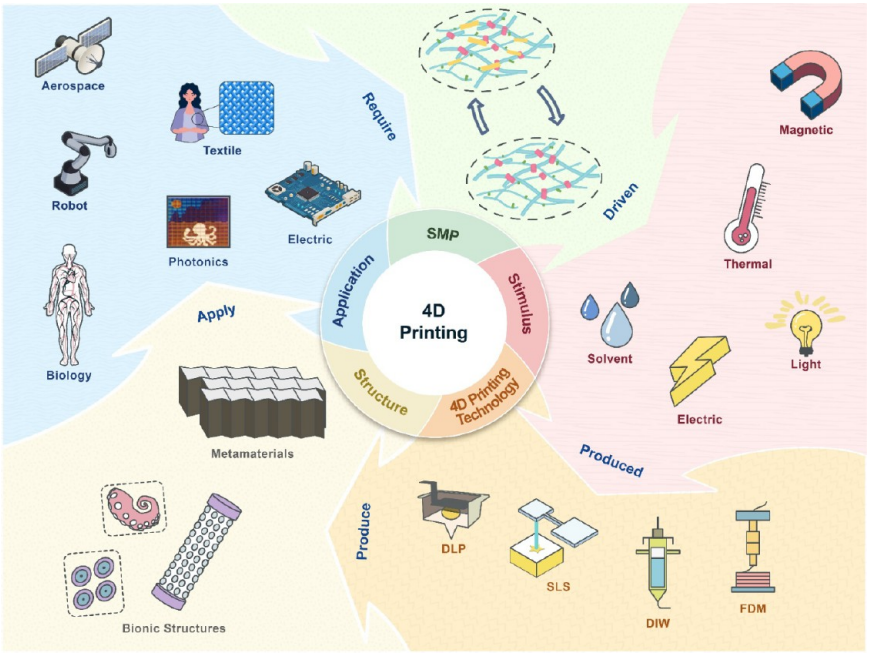

Figure 1. Schematic of 4D printing: mechanisms, actuation methods, printing technologies, structures, and applications of shape memory polymer materials.

or chemical agents) by altering intrinsic properties, such as shape or color. These materials serve as a bridge between 3D and 4D printing paradigms. In essence, 4D printing can be conceptualized as the 3D printing of smart materials. Among these materials, shape memory polymers (SMPs) have garnered significant scientific interest owing to their versatile applications and exceptional adaptability. These unique characteristics position smart materials as critical enablers for technological innovation across high-tech sectors, including biomedicine, architecture, automotive engineering, and robotics, providing a robust foundation to drive industrial advancement.

Currently, 4D printing technology is widely implemented across diverse sectors, with the most notable applications in aerospace and biomedicine.[22,23] In aerospace engineering, 4D printing is primarily utilized to fabricate mission-critical components for complex and extreme environments, such as space-deployable structures (e.g., hinges,[2] trusses,[24] and solar arrays[25]), release mechanisms for payload deployment,[26] and morphing aircraft configurations capable of adaptive aerodynamic optimization.[27] By integrating lightweight and high-strength smart materials, 4D printing significantly enhances the performance-to-weight ratio of aerospace systems, thereby meeting stringent industry demands. In biomedical applications, 4D printing enables patient-specific customization. Notable advancements include drug delivery systems that achieve time- and site-specific pharmaceutical release under minimally invasive conditions,[28] improved therapeutic precision while reducing patient discomfort, and self-expanding stents that adapt morphologically to intricate anatomical structures, thereby enabling highly personalized medical interventions.[29]

Although various smart materials have been employed in 4D printing, their performance remains limited in aspects such as shape memory precision, deformation reversibility, material strength, and durability—constraints that must be addressed to meet increasingly demanding application requirements. From a technical perspective, significant challenges persist in achieving high-precision and high-efficiency multimaterial 4D printing, particularly regarding material compatibility, interfacial bonding strength, and precise material switching/control during the printing process. These limitations hinder the broader application of 4D printing in the fabrication of sophisticated multifunctional structures. Furthermore, 4D printing requires novel design theories and methodologies to fully exploit its manufacturing advantages across spatiotemporal dimensions. This paper provides a comprehensive overview of 4D printing, as illustrated in Figure 1. It examines a range of intelligent materials applied in 4D printing technology, including both single-component smart materials and composites, offering a comprehensive analysis of their characteristics and application advantages. Subsequently, special emphasis is placed on the technological framework of 4D printing, offering a detailed interpretation from multiple perspectives, including its unique process principles, technical workflows, critical technological nodes, and innovative breakthroughs compared to conventional printing technologies. Finally, the discussion explores the principal application domains of 4D printing, highlighting its functional roles across different industries and scenarios while demonstrating its broad application prospects. This comprehensive approach aims to elucidate the multidimensional value and immense significant potential of 4D printing technology.

2. SHAPE MEMORY POLYMERS AND THEIR COMPOSITE MATERIALS

Smart materials serve as crucial bridges, enabling the transition from 3D printing to 4D printing. In the realm of 4D printing, the main single-component smart materials can be classified into three categories: shape memory polymers,[30] shape memory alloys,[31,32] and shape memory ceramics.[33] Compared with their metallic and ceramic counterparts, SMPs demonstrate superior advantages, including diverse stimulus responsiveness and exceptional deformation capacity.[15] Consequently, 4D printing research has predominantly focused on SMPs, and this section specifically concentrates on relevant information regarding these polymers. Furthermore, an

https://doi.org/10.1021/acsapm.5c02816
ACS Appl. Polym. Mater. 2025, 7, 14015−14032

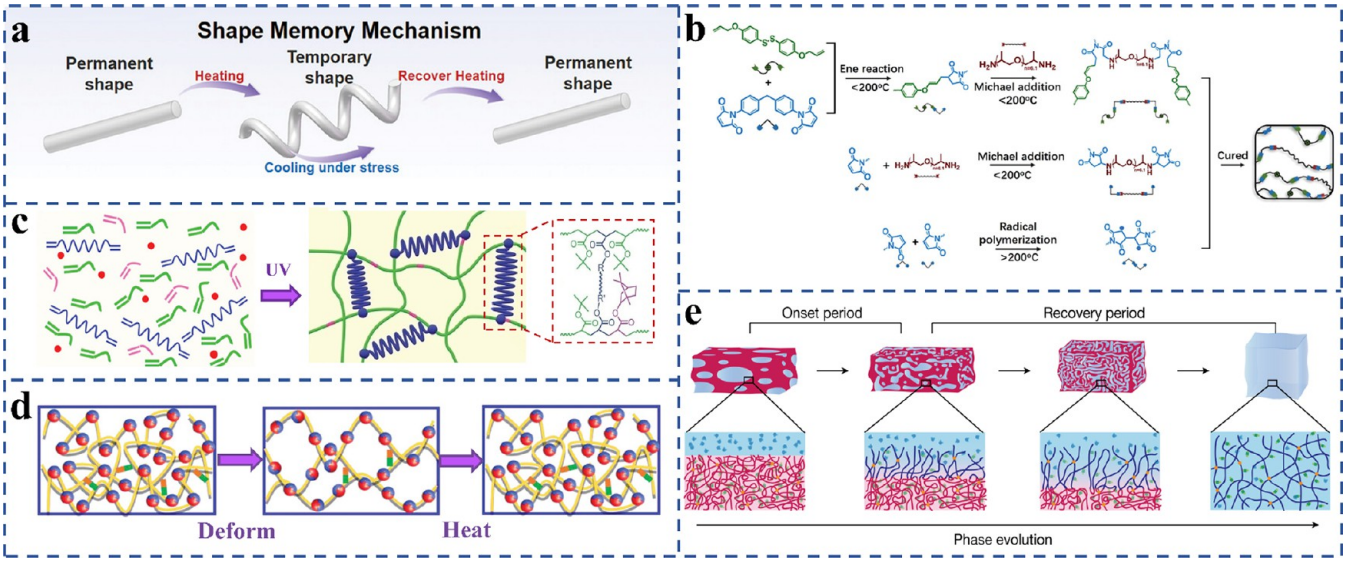

Figure 2. Unidirectional dual-SMPs: (a) Schematic of the shape memory mechanism.[39] Copyright© 2023 Wiley. (b) Reaction process of the BDM +DPS+D400 resin system.[36] Copyright© 2023 Wiley. (c) 3D-printed tBA-AUD SMP cross-linked network.[37] Copyright© 2022 Wiley. (d) Schematic of the thermoplastic polyurethane shape memory process.[38] Copyright© 2022 Wiley. (e) Phase transition mechanism of programmable recovery-initiation-time hydrogel.[28] Copyright© 2023 Nature.

increasing number of researchers are investigating composite materials containing additives, such as fibers and particles,[34] as well as those possessing renewable properties and self-healing capabilities, which will also be discussed in this section.

2.1. Shape Memory Polymers. Shape memory polymer is a polymer that can remember the shape of a previous object, which is embodied in the fact that when the shape memory polymer is in a temporary shape, an external stimulus is applied to it, and it returns to its original shape.[35] The realization of the shape-memory functionality involves two distinct phases. As illustrated in Figure 2a, the initial phase entails the programming process: the SMP is heated beyond its glass transition temperature (Tg), and then an external force is applied to deform it into a temporary shape. Subsequently, the material is cooled below Tg while maintaining deformation, after which the external force is removed. The second phase constitutes the recovery process, wherein appropriate stimulation induces the temporarily shaped SMP to revert to its original configuration.

To address the technological challenge of optimizing high-modulus tunability, self-healing capability, and reprocessability in thermosetting SMPs, Li et al. developed a novel bismaleimide (BMI)-based material system.[36] This system featured customizable elastic-to-rigid transitions, enabled via molecular structure design and dynamic covalent bond engineering, representing a significant advancement for sustainable 4D-printed smart structures. In this study, a diallyl ether- and disulfide-containing monomer (DPS) was synthesized via molecular engineering. It underwent a single-step reaction with 4,4'-bismaleimidodiphenylmethane (BDM) via steric hindrance effects to form a network structure with controllable cross-linking density. By incorporating diamine (D400) to modulate the molecular chain length (Figure 2b), the material achieved a static modulus spanning 3 orders of magnitude (1−506 MPa) and an ultrahigh Tg exceeding 153 °C, enabling continuous regulation from hyperelasticity to high rigidity. Furthermore, the dynamic exchange characteristics of disulfide bonds imparted the material with excellent self-healing capabilities and hot-press reprocessability, with the healed specimens retaining their shape-memory performance. This material system exhibited a broad processing window, superior thermal stability, and gradient temperature-responsive deformation via multimaterial integration—which are key attributes for 4D printing applications such as spacecraft recyclable structures and adaptive deployment mechanisms.

Conventional UV-cured SMPs for 4D printing are limited by insufficient mechanical strength, poor fatigue resistance, and restricted printing resolution. To address these challenges, Zhang et al. developed a mechanically robust UV-curable SMP material based on DLP technology, employing the synergistic design of high-performance cross-linkers and hydrogen-bonding interactions (Figure 2c), which offers high precision and enhanced durability.[37] The material utilized *tert*-butyl acrylate (tBA) as a linear chain-building unit and incorporated high-molecular-weight aliphatic polyurethane diacrylate (AUD) as a cross-linker. Precise control of the material properties was achieved by optimizing the component ratios. The developed tBA-AUD SMP system demonstrated exceptional stretchability up to 1240% strain at elevated temperatures in conjunction with excellent shape fixity, recovery ratios, and superior fatigue resistance. Mechanistic studies have attributed its high ductility to the long-chain characteristics of AUD cross-linkers and the dynamic rupture-reconstruction behavior of hydrogen bonds. This material is fully compatible with DLP printing technology, enabling rapid prototyping of complex geometries with 2-μm-level resolution. Furthermore, by integrating microfluidic channels and resistive heating elements, the researchers successfully demonstrated thermally actuated deformation capabilities in spacecraft deployable structures, such as foldable solar panels.

Through the synergistic engineering of dynamic oxime-carbamate bonds and hydrogen bonding interactions, Wang et al. developed a thermoplastic polyurethane material that integrates self-healing, photothermal responsiveness, and shape memory properties (Figure 2d).[38] The system employed polycaprolactone diol and isophorone diisocyanate as the polymer matrices, with 1,4-benzoquinone dioxime and 1,4-butanediol serving as dual-chain extenders. The self-healing capability was achieved via the reversible exchange of dynamic bonds. Under near-infrared (NIR) laser irradiation, the material exhibited high-efficiency photothermal conversion, significantly enhancing interlayer adhesion during printing and thereby resulting in a 320% increase in the tensile strength of vertically printed specimens.

Conventional shape-memory materials rely predominantly on external triggers, often resulting in uncontrollable recovery initiation times. To address this limitation, Ni et al. developed a 4D-printed shape-memory hydrogel with programmable recovery initiation employing phase separation and mass diffusion mechanisms (Figure 2e), enabling stimulus-independent smart deformation for applications such as implantable medical devices.[28] The photocurable hydrogel network, composed of acrylic acid and *N*,*N*'-methylenebis-(acrylamide), enables gradual modulus attenuation at 25 °C via calcium ion cross-linking and phase separation modulation. Unlike

https://doi.org/10.1021/acsapm.5c02816
ACS Appl. Polym. Mater. 2025, 7, 14015−14032

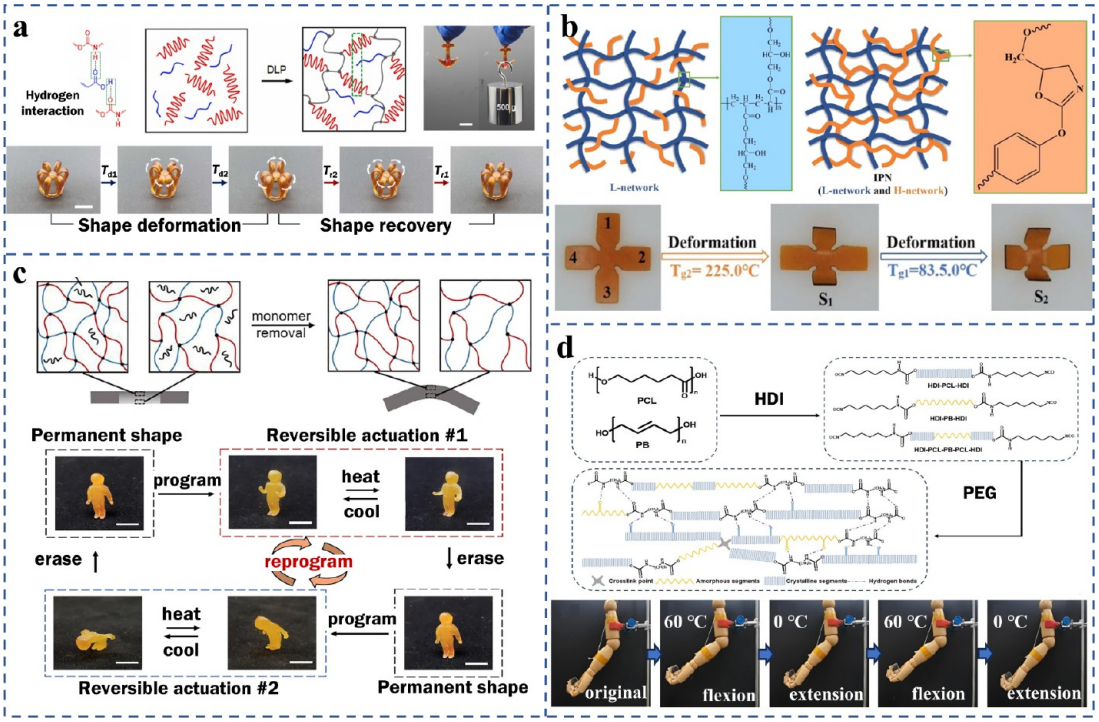

Figure 3. Triple-Shape and 2W-SMPs: (a) Schematic of sacrificial noncovalent hydrogen bond formation within printed networks and triple-shape memory mechanisms.[42] Copyright© 2022 Elsevier. (b) Network architecture in the sample and triple-shape memory programming-recovery cycles.[43] Copyright© 2023 American Chemical Society. (c) 4D printing mechanism schematic and reversible two-way shape memory demonstration via dual-programming modes using a 3D-printed animated cartoon figure.[45] Copyright© 2021 Elsevier. (d) Synthesis process of shape memory polyurethane (PU) and polymer network diagram, with bidirectional shape memory actuation emulating human arm flexion-extension.[46] Copyright© 2023 Elsevier.

conventional thermal-conduction-driven recovery, shape restoration was governed by internal water diffusion, with initiation times precisely tunable from 1 min to 24 h via programmed phase separation gradients. By integrating hydrogel "time locks" with thermally responsive SMPs, this mechanism can be extended to classical shape-memory systems, enabling multistage sequential deformation under single-temperature activation.

As previously discussed, SMPs capable of retaining only one temporary shape are termed as dual-SMPs, whereas those capable of retaining two temporary shapes are designated triple-SMPs.[40] The term "triple-shape" refers to a system comprising one permanent shape and two temporary configurations. On the molecular level, the highest number of temporary shapes that a polymer can record is determined by the number of distinct reversible phase transitions present in its structure. Achieving multishape memory effects requires the incorporation of additional reversible phase transitions, which pose significant scientific challenges.[41]

By incorporating noncovalent hydrogen-bond cross-linking mechanisms, Fang et al. developed a photocurable resin that exhibited exceptional mechanical properties and multishape memory effects.[42] A copolymer system of poly(urethane acrylate) and acrylic acid, wherein hydrogen bonds serve as sacrificial linkages, was employed to enhance material toughness. Notably, a single broad glass transition temperature spanning 70 to 150 °C enabled unique triple-shape memory behavior (Figure 3a). The experimental results demonstrated that the material, when programmed at distinct deformation temperatures, could sequentially recover two temporary shapes with shape fixity ratios (Rf) of 91.6% and 99.3% and shape recovery ratios (Rr) of 95.9% and 94.2%, respectively. This programmable multistage response mechanism, based on a single-phase transition, surpasses the limitations of conventional dual-shape memory materials and offers novel solutions for aerospace deployable structures, adaptive robotics, and other fields requiring complex deformation pathways.

Wang et al. developed a triple-shape memory material based on cyanate ester resin to address the demand for multishape memory smart materials in aerospace deployable structures.[43] This study employed a three-step fabrication method integrating DLP printing, UV curing, and thermal curing to construct an interpenetrating polymer network (IPN) structure. The resulting material exhibited two distinct Tg regions, enabling pronounced triple-shape memory effects (Figure 3b). This IPN system achieved a fracture strain of up to 10.9% and exhibited an enhanced fracture toughness. By integrating high strength, toughness, and multishape memory functionality, this strategy offers a promising solution for aerospace-deployable structures.

The shape-memory behavior described above operates via a unidirectional mechanism. After shape recovery, reprogramming is required to restore temporary shapes for subsequent actuation. In comparison, two-way shape memory polymers (2W-SMPs) are capable of spontaneously and reversibly transitioning between two different shapes when subjected to heating and cooling processes.[34] Current research on 2W-SMPs reveals the following focus distribution: 40% for actuators, 25% for medical applications, 8% for artificial muscles, and the remaining 27% for specialized domains such as drug delivery and smart grippers.[44] Furthermore, 2W-SMPs are categorized into force-dependent and force-independent systems based on whether external mechanical loading is required during deformation.

By integrating thiol-acrylate click chemistry with DLP technology, Shi et al. developed a reversible SMP based on dual-crystalline phases of polycaprolactone (PCL) and polypentadecalactone.[45] In this study, photocurable monomers polycaprolactone diacrylate and polypentadecalactone diacrylate were cross-linked via pentaerythritol tetra(3-mercaptopropionate) to construct an interpenetrating network with dual melting transitions. By controlling prestrain and UV exposure time, the material achieved a reversible strain of up to 20% with exceptional cyclic stability. A 3D-printed cartoon figure demonstrated reversible contraction/extension and posture changes under thermal stimulation (Figure 3c), exhibiting a room-temperature modulus of 100 MPa and a fracture elongation of 1200%, outperforming

https://doi.org/10.1021/acsapm.5c02816
ACS Appl. Polym. Mater. 2025, 7, 14015−14032

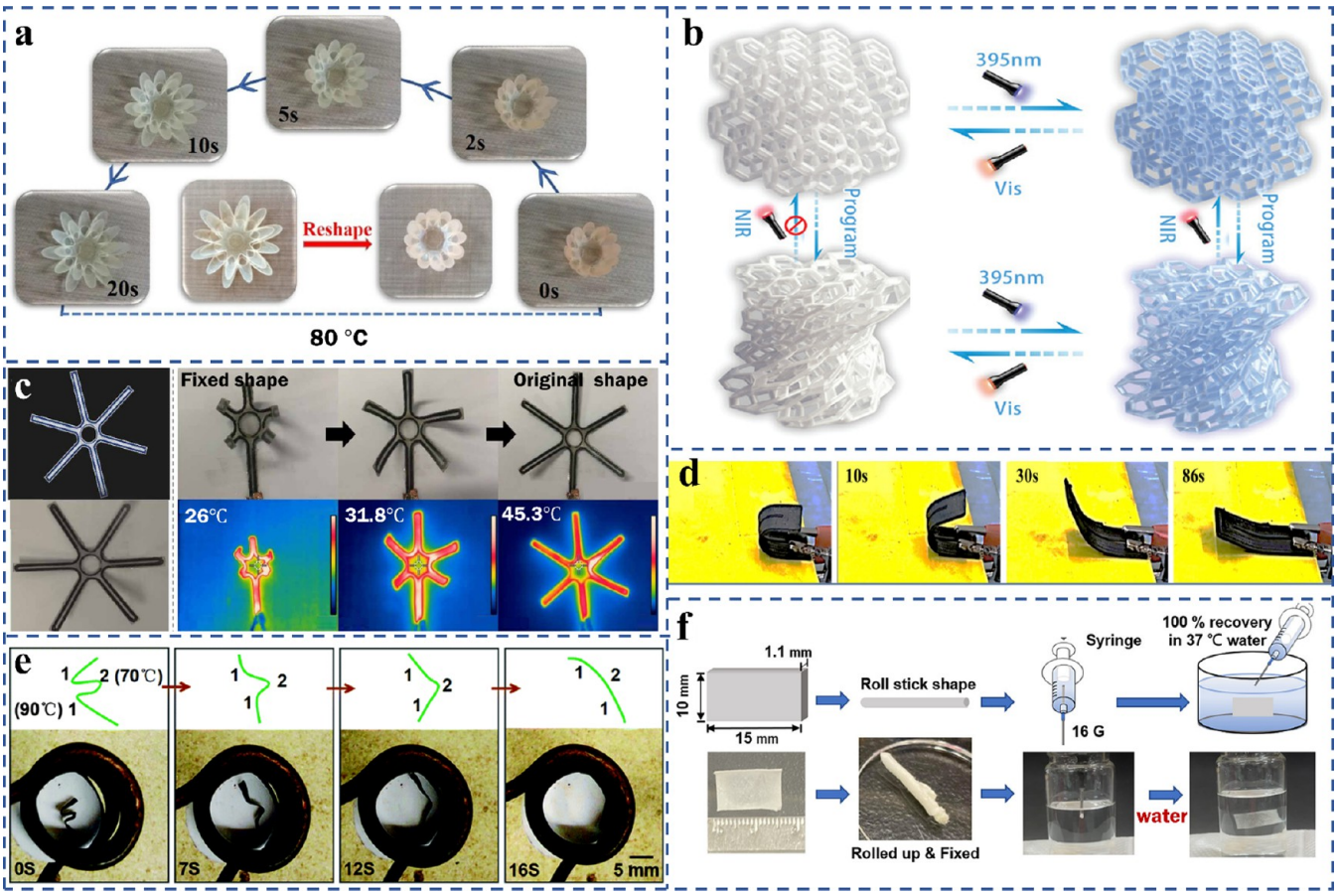

Figure 4. Composite SMPs with diverse actuation mechanisms: (a) Thermally driven floral shape memory behavior.[55] Copyright© 2022 Elsevier. (b) Visible-light-controllable photothermal properties of printed lattice structures.[56] Copyright© 2024 Wiley. (c) Snapshots and infrared images of a claw device based on CCF/PLA composite during electrothermal shape recovery.[57] Copyright© 2021 IOP Publishing. (d) Electrically driven shape memory cycle of PLA/CNT composites.[58] Copyright© 2022 Elsevier. (e) Magnetically induced triple-stage shape recovery process.[59] Copyright© 2015 the Royal Society of Chemistry. (f) Shape recovery of cryogels: a sheet-shaped cryogel rolled into a rod at 70 °C, fixed, and injected into 37 °C water to revert to its original form.[60] Copyright© 2022 American Chemical Society.

conventionally processed materials. This study addressed the limitations of single deformation pathways in traditional reversible SMPs by employing synergistic DLP fabrication and dual-phase crystalline design.

Conventional 2W-SMPs typically exhibit insufficient mechanical properties, which limit their applications in flexible electronics and soft robotics. To address this challenge, Guo et al. developed a stress-free bidirectional shape memory polyurethane material with ultrahigh toughness via a molecular spring strategy.[46] The study designed a cross-linked network comprising PCL, polyethylene glycol (PEG), and polybutadiene (PB) via a two-step polymerization process, where PB segments act as "molecular springs" to enable stress-free bidirectional shape memory effects through elastic energy storage and release mechanisms. The material demonstrated excellent integrated performance: tensile strain up to 2342%, true tensile strength of 591 MPa, and energy density and power density reaching 17.7 and 13.4 times those of human skeletal muscle, respectively. Under thermal stimulation, it achieved 13.7% reversible deformation without external stress, successfully emulating human elbow flexion and object grasping/releasing motions (Figure 3d). Furthermore, its superior cyclic stability and biocompatibility establish a foundation for biomedical applications, such as artificial ligaments.

With the growing demand for advanced materials, an increasing number of materials with unique properties and functionalities have been developed. These materials either address the limitations of their conventional counterparts or exhibit unprecedented capabilities, as exemplified by vitrimers[47] and self-healing materials.[48]

Plastics are generally categorized into two main types: thermoplastics[49] and thermosets.[50] Thermoplastics comprise polymer chains without chemical cross-links and rely on sufficient molecular weight to achieve intermolecular entanglement. In their molten state, the enhanced molecular mobility enables repeated melting and reshaping, offering versatility in terms of processing and recyclability. When heated above the Tg or melting temperature (Tm) of semicrystalline polymers, thermoplastics flow macroscopically as viscoelastic liquids. However, despite their recyclability, thermoplastics generally lack stability and crack resistance. In contrast, thermosetting materials undergo covalent cross-linking between the polymer chains. Under thermal or solvent-induced conditions, these chains result in a 3D network that restricts chain mobility, rendering the thermosets insoluble. Above Tg, thermosets exhibited no flow behavior. Compared with thermoplastics, thermosets demonstrate greater durability and enhanced stability in harsh environments but lack reprocessability.

Vitrimers combine the advantages of thermosetting and thermoplastic materials, bridging the conventional divide between the two polymer classes. These materials incorporate dynamic covalent cross-links that undergo associative exchange reactions without dissociation, achieving a balance between robust mechanical properties and processability. The term "vitrimer" was introduced by French scientist Ludwik Leibler. In 2011, Leibler et al. developed an epoxy-based vitrimer with a cross-linked network capable of topological rearrangement via exchange reactions without depolymerization.[51] When heated above the topological freezing temperature (Tv), the material

https://doi.org/10.1021/acsapm.5c02816
ACS Appl. Polym. Mater. 2025, 7, 14015−14032

exhibited sufficient ductility for reprocessing while retaining dimensional stability.

The synthesis of vitrimers primarily involves two approaches: the polymerization of multifunctional monomers and cross-linking of thermoplastics. The first strategy involves curing multifunctional monomer mixtures to construct networks containing dynamic covalent bonds. In step-growth polymerization, these dynamic covalent linkages may either form during network assembly or preexist in at least one monomer. The most straightforward method for chain-growth polymerization involves copolymerization with difunctional cross-linkers that incorporate dynamic covalent bonds. The second approach converts thermoplastics into vitrimers via two key pathways: one involves positioning functional groups capable of undergoing exchange reactions along the polymer backbone or as pendant side groups, and the other introduces dynamic functionalities during polymer synthesis via copolymerization with exchangeable comonomers. These functionalized thermoplastics are subsequently cross-linked in solution or molten state to form vitrimers. This methodology offers significant flexibility in customizing polymer matrices, dynamic bond types, and synthetic conditions, thereby enabling versatile material design.[52]

Self-healing materials play a critical role in reducing resource waste, extending product lifespans, enhancing mechanical system efficiency, and increasing reliability standards through intrinsic repair mechanisms.

In the 1970s, Malinskii et al.[53] pioneered the research on polymer self-healing, primarily focusing on polyvinyl acetate (PVAc). Self-healing polymers can be categorized into two classes: intrinsic and extrinsic systems. Intrinsic self-healing polymers rely on reversible reactions or chain mobility triggered by external stimuli (e.g., heat, light, or pH changes) to reorganize their internal microstructures, thereby achieving autonomous crack closure. In contrast, extrinsic self-healing polymers can be engineered by embedding microcapsules or hollow fibers containing healing agents in the polymer matrix. When microcracks propagate through the material, mechanical stress triggers the rupture of these microcontainers, releasing the encapsulated healing agents. Subsequent curing reactions (e.g., polymerization or cross-linking) of the released agents repair the damage and restore structural integrity.

2.2. Composite Materials. Composite materials are engineering materials composed of two or more constituent materials that have significantly different physical, chemical, and mechanical properties. While these constituents retain their individual characteristics within the composite, the resultant properties are not merely additive but demonstrate synergistic enhancement—achieving a "1 + 1 > 2" effect. In the composite architecture, one phase serves as a continuous matrix, whereas the other exists as a discrete reinforcement phase distributed uniformly throughout the matrix. These phases maintain distinct interfaces while functionally interacting with each other.

The actuation mechanisms of SMPs are intrinsically linked to the selection of the reinforcement phases. The actuation modes of the SMPs can be strategically modulated by incorporating diverse reinforcement materials into the matrix. The SMP actuation modalities are typically categorized as temperature-, light-, electric field-, magnetic field-, or solvent-driven systems.

Thermal stimulation is the most prevalent actuation method.[54] When heated above Tg, the SMPs recover their permanent shapes. Wang et al. developed an IPN epoxy composite via UV postcuring and gamma ray irradiation synergy, which demonstrated precise thermal responsiveness.[55] The temperature-gradient-triggered shape memory effects exhibited excellent efficiency: under 80 °C stimulation, a 4D-printed chrysanthemum petal structure transitioned from a closed temporary state to its original open configuration within 20 s, whereas a complex twisted vessel structure achieved full shape recovery in 5 s (Figure 4a). Experimental results demonstrated that the temperature-regulated cross-linking network, synergized with short glass fiber reinforcement, not only provided a high storage modulus but also significantly improved thermal stability.

Compared with other stimuli, light irradiation offers unique advantages in terms of remote and localized actuation control. Light-driven SMP actuation operates by employing two primary mechanisms: (1) photochemical transformation via light-responsive functional groups and (2) photothermal conversion, wherein light energy is transduced into thermal energy to trigger shape recovery.

Feng et al. developed a light-switchable shape-memory nanocomposite by incorporating $WO_{2.9}$ nanoparticles (Figure 4b), achieving high-precision fabrication of complex architectures via DLP-based 4D printing.[56] The material combined UV-curable shape-memory resin with trace $WO_{2.9}$ particles, exhibiting exceptional photothermal conversion efficiency (η>78%) and reversible photochromic behavior, which sustains over 50 reversible deformation cycles without performance degradation. The printed structures exhibited rubber-state tensile strains exceeding 1000% with superior fatigue resistance, spatially programmable actuation zones, and remote infrared activation capabilities. This study significantly advanced the applicability of light-triggered shape-morphing systems to smart wearables, microactuators, information encryption, and spacecraft reconfigurable structures.

Electrically driven actuation has attracted significant research interest, owing to its rapid response and precise controllability. Current studies of electric-field-stimulated SMPs have predominantly focused on shape memory composites (SMCs). By uniformly incorporating conductive fillers—such as carbon nanotubes (CNTs), carbon black, graphene, or metal nanoparticles—into the SMP matrix, a continuous conductive network is formed within the material, imparting the SMCs with electrical conductivity.[54] Based on the morphology of the functional fillers, SMCs can be categorized into particulate-filled, fiber-reinforced, nanopaper-reinforced, and hybrid filler systems.

Chen et al. investigated the electrothermal shape memory behavior of 4D-printed continuous carbon fiber/polylactic acid (PLA) composites.[57] This study demonstrated the exceptional performance of these SMCs under electrothermal activation, particularly in enhancing their mechanical strength and shape recovery efficiency (Figure 4c). The incorporation of continuous carbon fibers significantly improved the mechanical properties of the composite while enhancing its shape-recovery capability. Under electrothermal stimulation, the composite achieved a 90% shape recovery ratio with a maximum recovery force of 7.38 N.

Dong et al. developed a 4D-printed electroactive shape-memory structure based on PLA/CNT composites.[58] This study fabricated composite filaments with 5 and 8 wt % CNT via FDM and systematically analyzed their electrical conductivity, thermal properties, and shape-memory behavior (Figure 4d). The experimental results revealed that the 8 wt % CNT composite achieved an electrically induced shape recovery ratio of 95%. The synchronized actuation of complex geometries, including pyramidal and rhombic structures, was successfully demonstrated through an optimized infill orientation. The rhombic-lattice external fixator prototype achieved 90% deformation recovery within 60 s under 20 V of activation. This study provides novel insights into the 4D printing of electroactive devices employing synergistic process-structure optimization, with significant potential for use in programmable soft actuators and adaptive medical implants.

Magnetically driven shape memory effects are achieved by incorporating magnetic fillers, such as iron oxide, nickel powder, or neodymium−iron-boron (NdFeB) alloys. Magnetic fields penetrate most materials noninvasively, offering a safe and efficient actuation methodology.

Therefore, Zhang et al. developed a magnetically driven multishape memory composite using Nafion/Fe_3O_4 nonwoven fibers.[59] A composite film fabricated via electrospinning with Fe_3O_4 nanoparticles embedded in Nafion fibers exhibited multistage shape memory effects (Figure 4e). Rapid actuation was achieved via magnetically induced internal Joule heating, while the surface temperature remained below 40 °C to ensure biosafety. By programming the temperature gradients and magnetic field intensities, the material sequentially recovered up to four temporary shapes with transition times under 18 s, demonstrating shape fixity and recovery ratios exceeding 90%. The innovation lies in its magnetothermal self-

https://doi.org/10.1021/acsapm.5c02816
ACS Appl. Polym. Mater. 2025, 7, 14015−14032

regulation mechanism, which enables precise thermal zone control without the thermal damage risks inherent in external heating methods. In addition, the retained porous structure ensured breathability and biocompatibility.

Aqueous solutions dominate solvent-driven actuation systems, although ethanol, hydrochloric acid, and ethyl acetate are occasionally used. The inherent presence of interstitial fluids and blood in biological organisms renders solvent-responsive materials to be particularly suitable for biomedical applications.

Juan et al. proposed a liquid-responsive smart material system.[60] They synthesized self-healing hydrogels and shape-memory cryogels by functionalizing cellulose nanofibers (MCNFs) as cross-linkers, which were chemically integrated with glycol chitosan (GC) via dynamic Schiff base bonds. In a 37 °C aqueous environment, the cryogel exhibited a unique liquid-actuated behavior: its macroporous structure resulted in rapid absorption of water and swelling, achieving shape recovery via MCNF crystalline reorientation (Figure 4f). This solvent-responsive mechanism was validated by employing in situ SAXS/WAXS analysis, demonstrating that water infiltration-induced hydrogen bond reorganization and dynamic crystalline domain alignment governed the deformation. Furthermore, the shear-thinning behavior of the hydrogel enables precise injectable molding in liquid media, whereas the rapid hygroscopic expansion capability of the cryogel enables in situ adaptability to moist biological environments.

3. 4D PRINTING TECHNOLOGY AND 4D-PRINTED STRUCTURES

3.1. 4D Printing Technology. Several 3D printing technologies have been developed to process a range of materials, including metals, polymers, ceramics, and their composites. 4D printing integrates 3D printing with shape memory functionality, and its core innovation is rooted in the selection of materials that exhibit shape memory or self-adaptive properties. These materials enable preprogrammed structural transformations in response to external stimuli. Based on material characteristics, 4D printing methods can be categorized as FDM,[61] DIW,[62] SLS,[63] and VP.[64]

3.1.1. Fused Deposition Modeling (FDM). FDM is one of the most extensively utilized 3D printing technologies and is valued for its affordability and ease of operation. In FDM, thermoplastic filaments (e.g., PLA, PC, ABS) are heated to a molten state and extruded through a micronozzle. The extruded material is rapidly cooled and solidified in ambient air to form a stable structure. By programmatically controlling the extrusion coordinates on the build platform, these layers are sequentially deposited to fabricate three-dimensional objects.

Modifications to conventional FDM techniques can significantly enhance the shape memory performance. Zhou et al. proposed a coextrusion 4D printing (CE-4DP) strategy for fabricating smart materials by embedding continuous metallic fibers (CMFs) in high-performance SMPs to achieve rapid and precise selective deformation control.[65] Their study demonstrated the synchronous printing of $Cr_{20}Ni_{80}$ fibers with polyether ether ketone (PEEK) to form composite structures (Figure S1a). Localized electrical heating via the Joule effect effectively addresses the inefficiency and global heating limitations inherent in conventional thermal actuation methods.

3.1.2. Selective Laser Sintering (SLS). SLS is a powder-based additive manufacturing method that utilizes one or more lasers to selectively melt and fuse particles on a surface within a sealed chamber.[7] After the particles are sintered, the unsintered powder is removed to obtain the final product. Compared with other fabrication processes, SLS enables multimaterial composite sintering and support-free fabrication, making it suitable for producing components with complex internal cavities and lattice structures.

Wu et al. developed a magnetic-responsive 4D printing system based on SLS, fabricating a remotely controllable magnetic-driven gripper using $Nd_2Fe_{14}B$ magnetic particles compounded with thermoplastic polyurethane.[66] Their approach leveraged SLS to achieve a uniform dispersion of magnetic particles within the polymer matrix, followed by postmagnetization to impart permanent magnetism to the printed structures (Figure S1b). SLS-fabricated magnetic composites exhibit both high mechanical strength and noncontact remote actuation capabilities, offering novel solutions for scenarios requiring noninvasive manipulation, such as soft robotics and space-deployable structures. This study broadens the scope of 4D printing to multiphysics-coupled design frameworks.

3.1.3. Direct Ink Writing (DIW). DIW is an additive manufacturing technique that leverages the rheological properties of inks. A computer-controlled nozzle extrudes the ink material on demand and rapidly solidifies it upon deposition to form 3D structures layer by layer. DIW exhibits significant versatility for high-density materials such as liquid crystal elastomers (LCEs), epoxy resins, hydrogels, and metallic materials, demonstrating the advantages of multimaterial compatibility.[67]

Jiang et al. employed DIW technology with a customized printhead to achieve the synchronous deposition of continuous fibers and LCE resin through a customized printhead (Figure S1c).[68] Their open-chamber design replaced conventional sealed structures by utilizing shear flow fields generated by fiber traction to dynamically regulate the mesogenic monodomain alignment. Combined with UV in situ curing, this method successfully embedded carbon fibers, polyester fibers, and conductive fibers into the LCE matrix, achieving fiber volume fractions of 6.7%−15.9%. By optimizing the DIW process parameters, a rapid response time of 15 s was achieved under 80 °C activation. The composite exhibited enhanced mechanical properties, and the incorporation of conductive fibers increased the electrically induced deformation force by 133%.

3.1.4. Vat Photopolymerization (VP). Photopolymerization-based 3D printing utilizes light sources to initiate polymerization reactions in photosensitive resins, wherein monomers or oligomers cross-link into highly interconnected polymer networks.[69] Compared with other 3D printing methods, this technology offers rapid fabrication[70] and an exceptional surface finish.[71] The major photopolymerization techniques include stereolithography (SLA),[72] digital light processing (DLP),[73] and continuous liquid interface production.[74]

Cui et al. leveraged DLP technology to achieve high-resolution, reprogrammable 4D printing utilizing photocurable polythiourethane ink embedded with dynamic thiocarbamate bonds (TCBs) (Figure S1d).[71] These TCBs undergo topological rearrangement at 150 °C, enabling self-healing, hot-press reprocessing, and permanent shape reconfigurability, thereby overcoming the single-cycle deformation limitations of conventional SMPs. The printed material exhibited high mechanical strength and thermal stability, sustaining reversible grasp-release cycles under 500 g loads. By incorporating CNTs, the material gained NIR photoresponsiveness, achieving localized deformation control and a dual-mode-responsive

https://doi.org/10.1021/acsapm.5c02816
ACS Appl. Polym. Mater. 2025, 7, 14015−14032

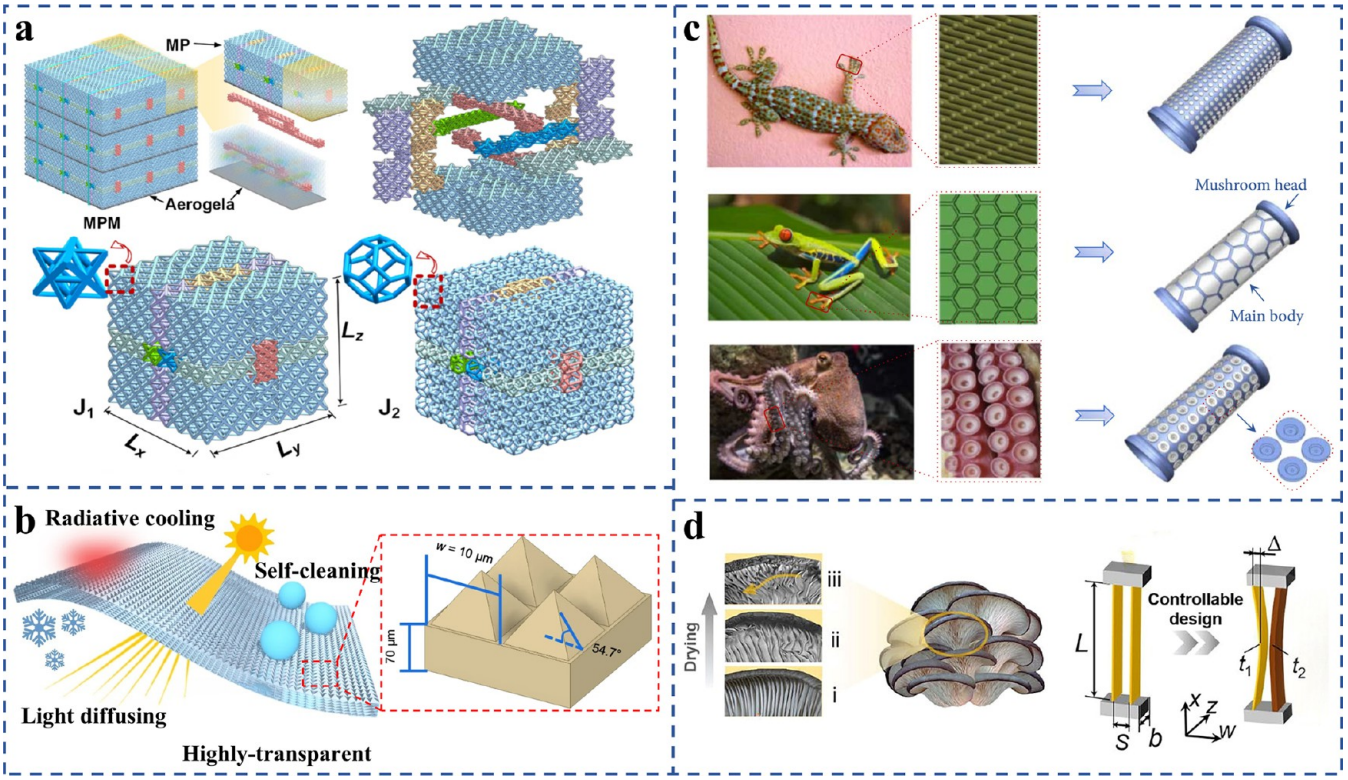

Figure 5. Metamaterials and bioinspired structures: (a) Multifunctional pixelated metamaterials (MPMs) composed of lightweight metamaterial units with customizable configurations.[81] Copyright© 2025 Elsevier. (b) Micropyramids-structured metamaterial integrating light diffusion, antireflection, self-cleaning, and radiative cooling functionalities.[83] Copyright© 2024 Nature Communications. (c) Colon stent designs inspired by gecko, tree frog, and octopus adhesion mechanisms.[89] Copyright© 2022 American Association for the Advancement of Science. (d) High-load-capacity snap-through metamaterial (STM) units inspired by mushroom gill folds.[91] Copyright© 2024 Elsevier.

smart alarm system that reacts synchronously to thermal and optical stimuli.

3.2. 4D Printing Structures. The 4D printing technology is advancing structural engineering into a new era with transformative potential. Unlike traditional 3D printing, which constructs objects in three-dimensional space, 4D printing incorporates a time-dependent dimension, enabling printed structures to dynamically alter their form and properties in response to environmental stimuli or temporal evolution. The essence of this technology lies in its ability to precisely control material behavior under external triggers, thereby fabricating complex architectures with tunable metamaterial properties and bioinspired structural features.

3.2.1. Metamaterials. Metamaterials are artificially engineered functional materials exhibiting excellent physical properties that surpass those of natural materials, achieved through periodic or aperiodic structural arrangements.[75] This concept was first proposed by Walser to describe three-dimensional synthetic composites with periodic structures that are not found in nature. By rationally designing ordered architectures at critical physical scales, metamaterials exhibit extraordinary properties that are not attainable by conventional materials, such as negative permeability and permittivity,[76] auxetic behavior,[77] and zero refractive index.[78] Under loading, their designed unit cells collectively emulate the macroscopic response of a new material, demonstrating unique mechanical performance. Consequently, the material properties—including permeability, permittivity, refractive index, and elastic modulus—are determined by the geometric configuration of the structures and meta-atoms.[79] Therefore, the choice of manufacturing technology is critical for achieving optimal metamaterial functionality.

In this context, additive manufacturing has emerged as a transformative solution that enables the fabrication of complex metamaterial structures, which are challenging or impossible to produce using conventional methods.[80] Recent advances in additive manufacturing have accelerated progress in the electromagnetic, acoustic, and mechanical applications of metamaterials, in addition to expanding design flexibility and innovation potential. Building on this foundation, researchers have integrated 3D printing with smart materials to pioneer innovative approaches for mechanical metamaterials. 4D printing introduces time-dependent dynamic capabilities into static 3D-printed structures, enabling controlled transformations in morphology, properties, and functionality under specific external stimuli. By imparting mechanical metamaterials with adaptive intelligence that is responsive to environmental changes, 4D printing has significantly enhanced the design freedom of metamaterial systems.

Leveraging 4D printing technology, Xin et al. developed a mortise-and-tenon-inspired mechanical-electromagnetic multifunctional pixelated metamaterial (MPM).[81] Inspired by traditional Chinese architectural joinery, this design employs a modular assembly of discrete mortise-and-tenon components to achieve reconfigurable, repairable, and scalable manufacturing (Figure 5a). Drawing on the flexible constraint mechanism of Hanfu-silk ribbons, a ribbon-like binding strategy was proposed to transfer mechanical loads while suppressing cross-pixel damage. The metamaterial unit integrates lightweight lattice structures with MXene@GO composite aerogels,

https://doi.org/10.1021/acsapm.5c02816
ACS Appl. Polym. Mater. 2025, 7, 14015−14032

forming a "brick-mortar" hybrid architecture that combines high specific strength with exceptional electromagnetic wave absorption. This structure−function-integrated approach offers lightweight, self-healing, and multifunctional solutions for aerospace electromagnetic stealth applications.

Also inspired by traditional Chinese mortise and tenon structures, Yan et al. designed a novel honeycomb acoustic metamaterial with enhanced mid- to low-frequency noise absorption.[82] By incorporating the interlocking principle of ancient wooden joinery into a hexagonal cell design, this study overcomes the low-frequency performance limitations of conventional honeycomb absorbers via micropore position modulation and tenon geometry optimization. The experimental results demonstrated a 10 Hz reduction in resonance frequency compared with traditional honeycombs, with dynamic tuning of resonance frequencies (15%−30%) achieved by adjusting the tenon length and micropore alignment. The distinctive mortise-tenon coupling mechanism extended the thermal-viscous dissipation pathways, increasing the energy dissipation intensity by 40% when the micropores were adjacent to the tenon edges. This innovation effectively broadened the absorption bandwidth in the 400−800 Hz range. The proposed topology optimization strategy, while maintaining a thin panel thickness and shallow cavity depth, provides a groundbreaking solution for low-frequency noise control in high-speed trains and aircrafts, demonstrating the synergy between traditional architectural wisdom and modern additive manufacturing.

Yengannagari et al. developed a transparent, self-cleaning multifunctional structure based on polymeric microphotonic metamaterials via micron-scale pyramidal surface engineering, achieving synergistic control of light-thermal-hygroscopic multiphysical fields.[83] The metamaterial utilizes a polydimethylsiloxane (PDMS) substrate with high-density micropyramid arrays on its surface (Figure 5b). A multistage reflection mechanism enhances the visible light transmittance to 95% while achieving 73% diffuse transmittance, effectively suppressing glare and optimizing indoor light distribution. The micropyramid structures induce electric dipole resonance coupling in the 8−13 μm wavelength range, enabling near-blackbody-level infrared emissivity with a radiative cooling power of 97 W/m^2 and a temperature reduction of 6 °C under 63% humidity. Inspired by the microcone geometry of lotus leaves, this material exhibits superhydrophobicity and incorporates dynamic wettability modulation on microstructured surfaces to enable dual-mode self-cleaning via active rainwater flushing and passive dew condensation, thereby addressing the limitations of conventional glass in optical regulation, thermal management, and durability.

Furthermore, using 4D printing technology, Xin et al. proposed a pixelated mechanical metamaterial (PMM) that overcomes the performance constraints of traditional tension-twist coupling metamaterials (TTCMs).[84] In this study, bioinspired helical microstructures were integrated with mechanical pixel (MP) arrays to achieve programmable and reconfigurable properties. By introducing a bioinspired helical ligament design emulating collagen fibers, the MP units demonstrated a deformation-mode transition from bending-dominant to stretching-dominant under tensile loading, significantly enhancing the tension-twist coupling effects and extending the maximum tensile strain to 60.91%, substantially exceeding the deformation capacity of conventional TTCMs. The unique pixelated architecture, comprising independent MP unit arrays, eliminates the interunit kinematic coupling constraints. This enables the dynamic adaptation of stress−strain curves and torsion angles via thermal stimulation of the temporary geometric parameters of the SMPs.

3.2.2. Bioinspired Structures. To endure ubiquitous natural challenges, organisms have evolved a wide range of structural adaptations for predation, camouflage, and locomotion. These biological blueprints have inspired researchers to design novel architectures exhibiting exceptional mechanical performance,[85] energy absorption capacities,[86] and superhydrophobicity.[87]

Deng et al. developed a 4D-printed composite material by embedding nanohydroxyapatite into a shape-memory polyurethane matrix, achieving both mechanical strength and body-temperature-responsive behavior.[88] Inspired by the anchorage structure of mangrove roots, this scaffold was designed as a multilevel branched unit array. Under thermal stimulation, it rapidly recovers from a compressed temporary state to a preprogrammed permanent configuration, precisely aligning with the cartilage defect contours. Rheologically optimized printing parameters imparted the material with shear-thinning behavior during extrusion, ensuring the high-precision fabrication of bioinspired structures. This dynamic design addresses spatial constraints in traditional scaffold implantation and demonstrates the feasibility of minimally invasive tissue engineering, as validated by in vitro degradation and in vivo biocompatibility.

Furthermore, biological morphology has inspired innovative stent designs. Lin et al. proposed a multifunctional biomimetic colorectal stent modeled after high-adhesion organisms, such as octopus suckers, tree frog toe pads, and gecko foot hairs.[89] This study meticulously constructed stent surfaces with microscale features, including octopus sucker-like concavities and hexagonal arrays emulating tree frog toe pads (Figure 5c), thereby significantly enhancing the antimigration capabilities. Functionalization with graphene oxide imparted photothermal responsiveness, enabling localized temperature control under NIR light to ablate tumor cells and inhibit restenosis. This synergy between biomimetic microstructures and photothermal functionality resolves the performance trade-off between antitumor efficacy and antimigration in conventional stents. Additionally, the integration of a drug-eluting system achieves multimodal therapeutic mechanisms, advancing personalized treatment for malignant obstructions.

Zhang et al. introduced a novel lattice metamaterial exhibiting tunable mechanical properties by integrating a bioinspired design with advanced manufacturing.[90] Inspired by the S-shaped curvature of the human spine and the arched morphology of tortoise shells, this study innovatively modified the traditional octet lattice by replacing straight beams with curved beam structures to create spine-inspired octet-S and tortoise-shell-inspired octet-A topologies. The S-curved design of octet-S optimized the force transfer pathways between struts, enhancing the energy absorption capacity by 78%, whereas the arched architecture of octet-A improved the load-bearing strength via localized stiffness amplification. The experimental and simulation results demonstrated a uniform stress distribution in both configurations, effectively mitigating the stress concentration at the lattice nodes observed in conventional designs. By leveraging the temperature-sensitive behavior of SMPs, this metamaterial enables the dynamic switching of stiffness, energy absorption, and vibration damping via thermal field modulation in conjunction with fully reversible shape memory functionality.

https://doi.org/10.1021/acsapm.5c02816
ACS Appl. Polym. Mater. 2025, 7, 14015−14032

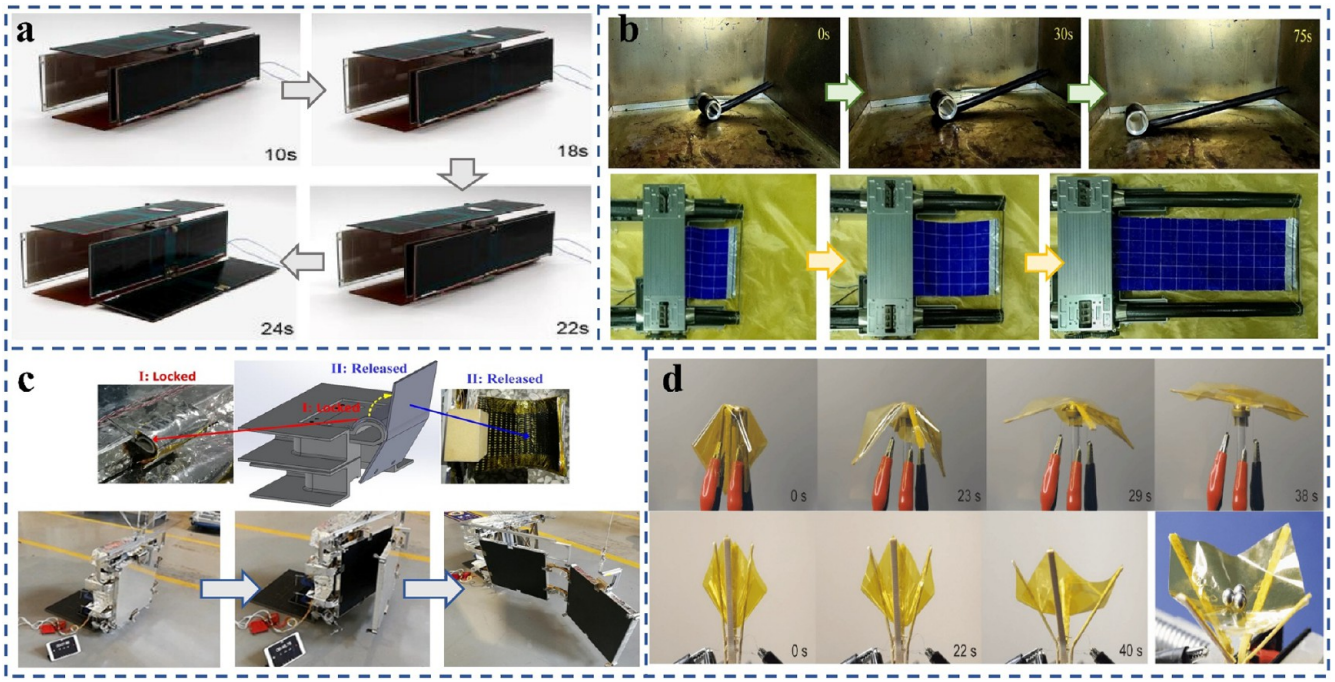

Figure 6. Applications of 4D Printing in Aerospace: (a) Solar panel deployment under 3 V DC voltage.[92] Copyright© 2020 Elsevier. (b) Deployment process of a coiled solar array.[93] Copyright© 2025 BioMed Central Ltd. (c) Release and deployment sequence of an intelligent solar array.[94] Copyright© 2025 American Institute of Aeronautics and Astronautics. (d) Drag sail deployment and bioinspired gripper with deployable joints based on shape memory PEEK.[95] Copyright© 2022 MDPI.

Inspired by the geometric frustration resulting from the drying-induced contraction of mushroom gills, Yan et al. developed a snap-through metamaterial (STM) (Figure 5d).[91] The design achieved an ultrahigh load-bearing capacity—55 times its own weight—via the axial compression of thin-walled strips and contact-induced stiffening mechanisms, while dissipating energy via geometry-triggered multistage buckling. The unique double-strip interlocking structure undergoes a multiphase deformation sequence-compression-contact-higher-order buckling-rapid rebound-generating reusable hysteretic damping with energy dissipation efficiency 60-fold higher than traditional bending-dominated metamaterials. This bioinspired approach overcomes the trade-off between load capacity and damping performance in conventional energy-dissipative materials. Furthermore, a preloading strategy enables adaptive attenuation of impact forces, offering a new paradigm for mechanical waveguides and soft robotic actuators.

4. APPLICATIONS OF 4D-PRINTED SHAPE MEMORY POLYMER COMPOSITES

4.1. Aerospace. In aerospace engineering, traditional structures are hindered by high weights and excessive volumes, which compromise mission efficiency. 4D printing technology is driving a paradigm shift toward lightweight and multifunctional designs. Using engineering structures capable of shape-shifting under specific conditions, this approach optimizes flight performance, reduces fuel consumption, and enhances spacecraft adaptability—creating new avenues for future space exploration.

Owing to payload volume constraints in launch vehicles, aerospace devices must maintain compact stowed configurations during launch and deploy postorbit insertion. Extreme operational environments demand exceptional reliability, whereas conventional mechanisms often face challenges, such as complex actuation and limited robustness. Zhang et al. developed an ultralightweight deployment mechanism for solar panels (Figure 6a), highlighting the potential of metamaterials in space applications.[92] This device employed fiber-reinforced SMPCs as the core material. Geometric parameter optimization achieved high locking forces with low stress concentrations, whereas screen-printed flexible redundant heating circuits enabled active thermal responsiveness. The integration of 77.8 dtex elastic fibers significantly enhances the toughness and shape recovery efficiency of the composite (η>92%) while preserving lightweight and low modulus properties. Additionally, a multimodal heating circuit design improves reliability via redundant layouts, addressing the failure risks of traditional resistive heaters under large-strain conditions. Thermal cycling and vibration tests validated stable locking performance and repeatable deployment capability in extreme environments.

Geometric optimization and multiphysics coupling mechanisms in smart materials represent critical frontiers in aerospace innovation. Xiao et al. proposed a thin-walled tubular deployable boom based on SMPCs for coiled solar array deployment in spacecraft (Figure 6b).[93] Featuring an open cylindrical cross-section, the boom optimizes the bending stiffness via radius, thickness, and opening angle adjustments guided by nonclassical composite beam theory, achieving a 23:1 compression ratio. Its novelty lies in coupling axial compression-induced contact stiffening with geometric contact buckling, enabling a three-phase transformation mechanism: "coiling-thermally triggered deployment-self-locking." Experiments demonstrate that the boom adaptively deploys flexible solar sails at a glass transition temperature of 80 °C, generating a peak driving force of 2.3 N. Furthermore, orthogonal testing confirmed the significant influence of the radius and opening angle on the driving force.

https://doi.org/10.1021/acsapm.5c02816
ACS Appl. Polym. Mater. 2025, 7, 14015−14032

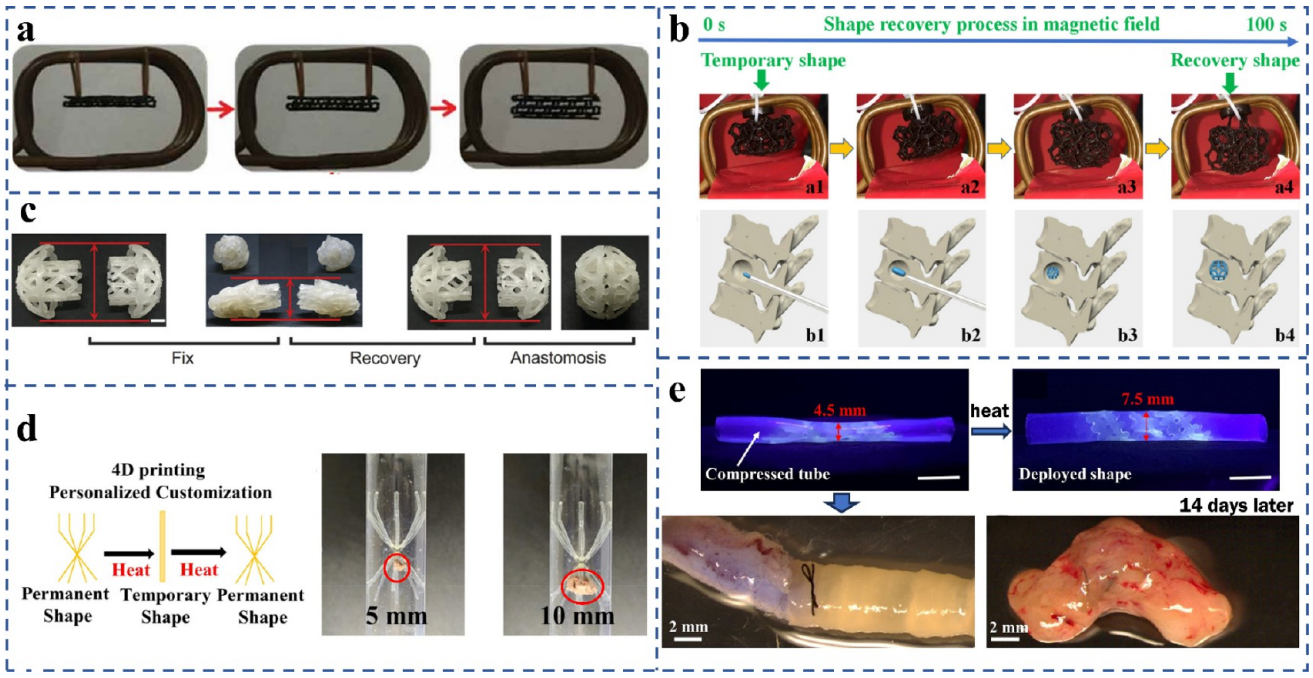

Figure 7. Applications of 4D Printing in Biomedicine: (a) Shape recovery process of a shape memory tracheal stent.[22] Copyright© 2021 Informa UK Limited. (b) Magnetic field-induced shape restoration behavior of 4D-printed bone repair structures.[98] Copyright© 2019 Elsevier. (c) Shape memory and anastomosis process of an intestinal anastomosis ring.[99] Copyright© 2023 Wiley. (d) Schematic of an inferior vena cava filter (IVCF) capturing thrombi.[100] Copyright© 2023 Elsevier. (e) Pre- and postimplantation images of a vascular stent anastomosed with murine aorta.[101] Copyright© 2021 Elsevier.

Lan et al. developed an intelligent solar array by integrating SMPCs with shape memory alloys (Figure 6c), eliminating the need for traditional pyrotechnic devices.[94] The core design employs SMPC hinges as actuation mechanisms and utilizes electrical heating to trigger shape recovery for a two-stage solar panel deployment. The self-locking mechanism ensures postdeployment stiffness and stability. The high compressive strain and low-temperature shock release of SMPCs, combined with the high locking force of SMAs, meet the high fundamental frequency requirements in the folded state while maintaining lightweight and reliability via iterative structural optimization.

Furthermore, Zhou et al. fabricated electrothermal-responsive metamaterial structures by embedding $Cr_{20}Ni_{80}$ conductive wires into a PEEK matrix via dual-extrusion 3D printing.[95] By modulating the density and distribution of conductive pathways, their design enables the precise control of localized temperature gradients, thereby optimizing shape recovery rates and actuation speeds. Customized structural parameters enhance strain energy storage efficiency, with recovery force increasing by 117% when thickness increases from 1.2 to 1.4 mm. The study also demonstrated the application of PEEK in bioinspired deployable structures such as electrically driven hinges for film drag sail deployment (Figure 6d), validating its stability in extreme environments.

4.2. Biomedicine. Over recent years, 4D printing technology has attracted considerable interest in the biomedical field. This is due to its ability to precisely create complex structures and its rapid response to stimuli. By creating implants and scaffolds capable of adapting to dynamic physiological environments, 4D printing enables personalized medical solutions tailored to individual patients.[96]

Zhang et al. have made significant strides in advancing the clinical translation of 4D printing and SMPs, addressing diverse therapeutic challenges ranging from respiratory diseases to bone regeneration.[97] To tackle tracheal stenosis, they developed a 4D-printed tracheal stent with bioinspired S-shaped hinges (Figure 7a).[22] Remotely triggered by magnetic fields or infrared light, the stent achieves 99% shape recovery within 40 s, while maintaining a strict maximum temperature limit of 58.7 °C to ensure therapeutic safety. The pore size and central angle of the stent were customized to align with the patient-specific tracheal morphology. Combined with the biodegradable properties of PLA/Fe_3O_4 composites, this design resolves the clinical limitations of traditional nickel–titanium alloy stents, such as migration risks and challenging removal. The "compressed implantation-in situ deployment" strategy offers a minimally invasive solution for airway stenosis.

Furthermore, leveraging the innovative design of magnetic PLA/Fe_3O_4 composites, Zhang et al. achieved rapid, magnetically controlled deployment of bioinspired bone scaffolds (Figure 7b).[98] The porous topology mimics the mechanical properties of natural bone tissue, while precise temperature regulation within the 40 °C physiological range promotes osteocyte alignment without the thermal damage risks associated with metallic implants. The scaffold, implanted in a compressed state, can be triggered by a 27.5 kHz magnetic field for deployment in situ, perfectly conforming to complex bone defect geometries.

Peng et al. developed a 4D-printed shape-memory intestinal anastomosis ring (Figure 7c) via FDM utilizing a PLA/poly(lactic-*co*-glycolic acid) (PLGA) blend.[99] By optimizing the PLA/PLGA ratio and incorporating a biocompatible plasticizer (acetyl tributyl citrate, ATBC), the Tg of the material was reduced to 43 °C, enabling rapid shape recovery in 50 °C warm water in conjunction with controllable degradation. A grid structure with a hook-locking mechanism enables a 50% diameter reduction in the compressed state for

https://doi.org/10.1021/acsapm.5c02816
ACS Appl. Polym. Mater. 2025, 7, 14015−14032

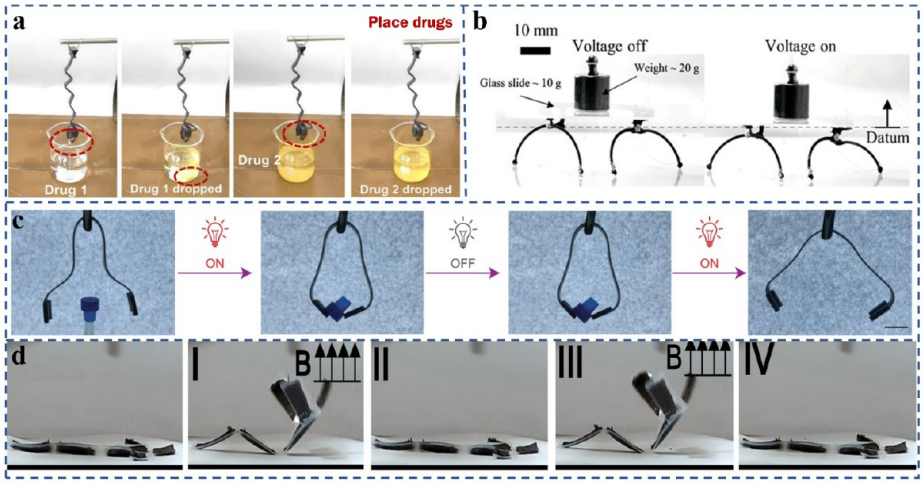

Figure 8. Applications of 4D printing in robotics: (a) Drug delivery by a 4D-printed soft robot under NIR light stimulation.[103] Copyright© 2023 Elsevier. (b) Actuated weightlifting robot lifting 313 times its own weight.[104] Copyright© 2022 Wiley. (c) NIR-controlled grasping and releasing of objects by a 4D-printed robotic gripper.[105] Copyright© 2023 Nature Communications. (d) Soft robot performing sit-up exercises under a magnetic field.[106] Copyright© 2024 Elsevier.

minimally invasive implantation, while achieving a postrecovery tensile strength of 35 N to meet the intestinal anastomosis requirements. Ex vivo porcine intestinal experiments validated the feasibility of thermally responsive deployment, mechanical locking, and degradation, thereby eliminating the need for secondary surgery.

Qu et al. designed a biodegradable inferior vena cava filter (IVCF) based on poly(glycerol sebacate acrylate)-*co*-hydroxyethyl methacrylate (PGSA-HEMA) via DLP.[100] By tuning monomer ratios, the transition temperature of the material aligns with physiological ranges while maintaining superior mechanical properties and shape recovery rates (η>95%). In vitro tests confirmed its cytocompatibility, hemocompatibility, and histocompatibility for implantation, with sufficient mechanical retention after 8-week degradation to intercept thrombi. Flow simulations demonstrated that the filter was able to recover its preset configuration at body temperature and completely trap 5−10 mm thrombi (Figure 7d).

Zhang et al. created a novel SMP using poly(glycerol dodecanedioate acrylate) (PGDA), with tunable transition temperatures (20−37 °C), suitable for 4D-printed bioadaptive vascular stents.[101] Photocurable modification overcame the printing limitations of thermosetting polymers, enabling complex 3D architectures, including overhanging "grids" and tilted "hollow cones." The printed stents exhibited exceptional shape memory performance (0.4 s recovery speed) and mechanical softening at body temperature, minimizing the mechanical mismatch with soft tissues. In vitro expansion of the compressed stents in a narrowed silicone tube (7.5 mm diameter) under thermal stimulation emulated angioplasty (Figure 7e). Following 14-day implantation in murine aortas, analysis revealed endothelialization, smooth muscle formation on the stent surface, and elastin deposition, underscoring the material's potential for bioadaptive vascular regeneration.

4.3. Robotics. Traditional robots lack autonomous adaptability, which limits their development in various applications. The advent of 4D printing has enabled robots to self-adjust and optimize based on task requirements, enabling them to operate adaptively in dynamic environments. This capability enhances robotic performance, survivability, and adaptability, particularly in complex scenarios.[102]

Gu et al. developed an SMP nanocomposite for soft robotics in hazardous environments utilizing a hydrogen-bonded metal-phenolic sacrificial network.[103] By doping Fe_3O_4 nanoparticles and optimizing the interfacial design, the material achieves high mechanical strength in conjunction with NIR and magnetic responsiveness. The multistimuli-responsive 4D printing of programmable soft grippers was realized via fused filament fabrication (FFF). The foldable structure and remote-triggering capability of the robots enable contactless drug delivery in hazardous chemical experiments, thereby mitigating operational risks (Figure 8a). The tests exhibited 98% shape fixation and 87% recovery rates over 15 cycles for a 1.5 mm-thick gripper arm, demonstrating reliability under harsh conditions.

Ferrer et al. addressed the stiffness limitations of conventional 4D-printed materials by developing multiscale heterogeneous polymer composites, achieving an elastic modulus 4 orders of magnitude higher than those of existing systems.[104] The composite combined tunable thermal expansion coefficients with electrical conductivity, enabling Joule-heating-driven self-sensing. Using this material, they designed electrically controlled bilayer structural units, creating a lifting robot capable of bearing 885 times its own weight and setting a record actuation stress of 6 MPa (Figure 8b). Furthermore, programming planar lattice structures enabled the autonomous deformation of self-supporting complex curvatures and multi-gait crawling robots, underscoring the potential for heavy-load transportation and adaptive architectures.

Liquid-metal composites have inspired novel designs for 4D-printed soft robots. Zhang et al. developed an NIR-responsive liquid metal−polymer composite by functionalizing liquid metal nanoparticles with reversible addition−fragmentation chain-transfer agents, enabling single-step synthesis and high-precision stereolithographic 3D printing.[105] By leveraging the photothermal conversion of liquid metal, the material recovered its preprogrammed shape within 60 s under 808 nm laser stimulation, retaining a 99% deformation recovery rate over 25 cycles. Compared with conventional rigid nanoparticle composites, the fluidic nature of liquid metal significantly reduces the glass transition temperature and tensile modulus, enhancing soft robot flexibility and

https://doi.org/10.1021/acsapm.5c02816
ACS Appl. Polym. Mater. 2025, 7, 14015−14032

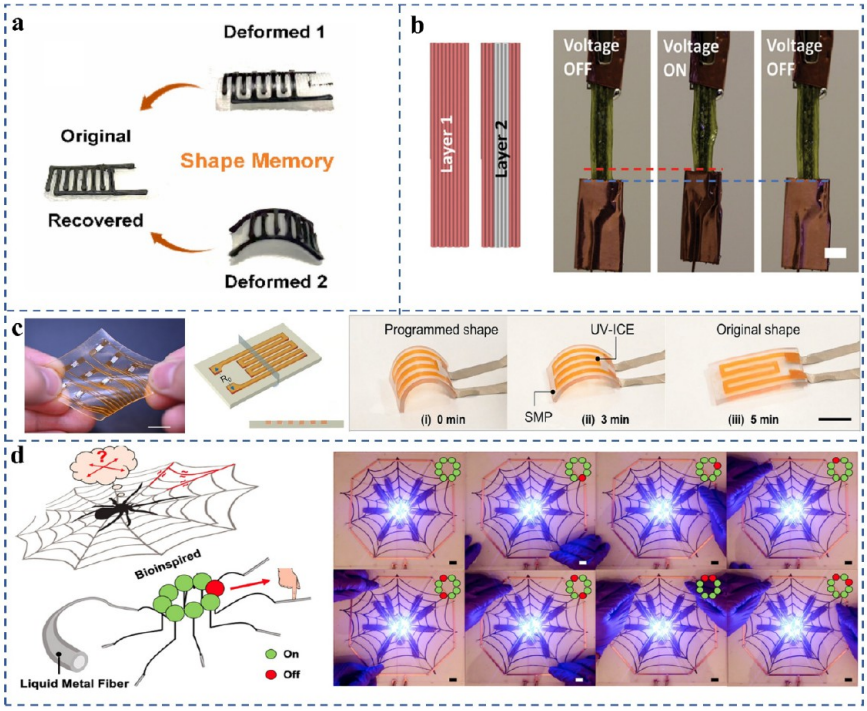

Figure 9. Applications of 4D printing in electronic devices: (a) Shape memory process of the 4D-printed tactile sensor (4DPS).[107] Copyright© 2023 Elsevier. (b) Voltage-activated transformation of the LM-LCE actuator, with blue and red dashed lines indicating macroscopic shape changes.[108] Copyright© 2020 American Chemical Society. (c) Shape memory process of the UV-ICE material.[109] Copyright© 2022 American Chemical Society. (d) A bioinspired robust sensor design: a highly stretchable EGaIn fiber acting as "spider silk" to transmit mechanical strain signals to a "nervous system".[110] Copyright© 2023 Elsevier.

deformation freedom without compromising the printing resolution (Figure 8c).

Additionally, Deng proposed a 4D printing strategy using photocurable magnetic hydrogels.[106] Bentonite was incorporated to improve the ink rheology and suppress magnetic particle agglomeration. In conjunction with capacitive discharge-assisted magnetic programming, this approach enabled the rapid fabrication of magnetic hydrogel structures without preprocessing. Under an external magnetic field, the material exhibits exceptional bending, grasping, and crawling capabilities. Magnetoresponsive deformation can be precisely controlled by adjusting neodymium iron boron (NdFeB) content and magnetic field strength (Figure 8d).

4.4. Electronic Devices. Traditional electronic devices, constrained by conventional manufacturing limitations, often lack the ability to autonomously adapt to environmental changes, thereby limiting their development and application. The integration of 4D printing technology into electronics has introduced a paradigm shift, enabling adaptive functionalities that improve device durability and user-friendliness, thereby offering innovative directions for next-generation electronics.

Ren et al. developed a 4D-printed tactile sensor (4DPS) employing a multimaterial extrusion process.[107] They used carbon black/PLA composites and shape-memory polyurethane to fabricate coplanar electrodes (Figure 9a). The adjustable detection range and sensitivity of the sensors stem from the thermal deformation of the SMPs, which alters the electrode height and spacing. By adjusting the printing parameters, the diameter of the coplanar electrodes can be precisely controlled, while the utilization of the thermal stress generated during printing enables 3D sensor configurations that are adaptable to curved surfaces. Additionally, 4DPS can be applied to nondevelopable surfaces, such as spheres and saddles, providing new avenues for environmental adaptation and self-adjusting test ranges in human−robot collaboration. This multifunctional 4D-printed tactile sensor is significantly promising for electronic devices, particularly adaptive sensing technologies and smart system integration.

Ambulo et al. reported a 4D-printable liquid metal-liquid crystal elastomer (LM-LCE) composite that responded to photothermal and electrothermal stimuli for shape morphing, which is applicable to soft robots and actuators.[108] By dispersing eutectic gallium−indium alloy (EGaIn) droplets into an LCE matrix, the composite exhibited NIR-induced photothermal responses at low liquid metal concentrations, achieving 150° bending under 800 mW/cm^2 irradiation. When the liquid−metal concentration was increased to 88 wt %, the EGaIn droplets formed conductive networks for electrothermal actuation (Figure 9b). This material retains both the compliance and shape-changing properties of the LCEs.

Based on DLP, He et al. utilized a multimaterial 3D printing technique to seamlessly integrate ultraviolet-curable ionically conductive elastomers (UV-ICE) with nonconductive materials to fabricate multifunctional flexible electronics with complex geometries.[109] The UV-ICE material developed by the team is highly stretchable and compatible with DLP technology, enabling the high-resolution fabrication of intricate 3D ion-conductive structures. By combining UV-ICE with nonconductive polymer substrates exhibiting varying mechanical properties, they produced resistive strain/force sensors, highly sensitive capacitive pressure sensors, and 4D-printed structures activated by ion-conductive circuits printed onto SMP substrates (Figure 9c).

https://doi.org/10.1021/acsapm.5c02816
ACS Appl. Polym. Mater. 2025, 7, 14015−14032

Xing et al. developed a metallic gel composed of copper particles, a eutectic gallium−indium alloy (EGaIn), and water.[110] This gel exhibited ideal rheological properties for room-temperature printing and achieved metallic conductivity without sintering. Three-dimensional printing was achieved at room temperature by adjusting the composition and pH to tune the rheology of the conductive solid−liquid−liquid suspension. Shear forces during printing induced anisotropic structures during drying, thereby enabling 4D printing. The printable metallic gel demonstrated excellent conductivity and temperature-responsive behavior, enabling the fabrication of complex conductive metal architectures (Figure 9d). This approach provides a new pathway for manufacturing electronic devices, particularly via room-temperature metal printing, and expands its applications in electronics and thermal and composite components.

4.5. Other Fields. With ongoing advancements in research and development, 4D printing technology has demonstrated significant potential for applications in food, homeware, and optical devices. By designing and manufacturing structures that respond to environmental changes, 4D printing can provide innovative solutions that drive progress across these domains. Zhang et al. proposed a 4D-printed electromagnetic architecture (EMA) with ultrafast shape deformation and high-sensitivity detection capabilities.[111] The EMA comprised 4D-printed polymer scaffolds, magnetic components, and conductive parts. Experiments indicate that the EMA exhibits extremely low shape deformation response times and highly sensitive external pressure detection (Figure S2a). This study represents the first report on such capabilities in current 4D printing research. Employing numerical simulations and parameter optimization, the study investigated the impact of unit cell structures on EMA performance and successfully built a "sensing-deformation" system that intelligently distinguishes objects for capture or release. This study accomplishes the efficient integration of ultrafast shape deformation with ultralow stress detection within 4D-printed architectures.

To enable the innovative development of functional foods, Zhu et al. applied a composite of betanin, gelatin, and nanoscale chitin to 4D-printed surimi products.[112] The composite protects betanin from high temperatures and UV light, enhancing its stability and improving the thermal stability, microstructure, and rheological properties of surimi. The 4D-printed surimi exhibited excellent color-changing characteristics based on solution pH variations, with reversible color changes, offering more dietary options and nutritional support for patients with swallowing disorders (Figure S2b).

Using two-photon polymerization lithography (TPL) technology with a half-pitch resolution of approximately 300 nm, Zhang et al. explored the 4D printing of SMPs at submicron scales, achieving time-responsive 3D structures.[113] The study developed a novel SMP photoresist material based on Vero Clear. Through manipulation of the geometry of cross-linked SMP structures, multiple structural colors were achieved with the rapid recovery of color and geometry enabled by the shape-memory effect (Figure S2c). The high-resolution printing and exceptional reversibility demonstrate significant potential for microtopology and optical properties with applications in temperature-sensitive labels, anticounterfeiting information hiding, and tunable photonic devices.[114]

Wang et al. proposed a 2.5-dimensional dynamic structural color based on heterogeneous nanogratings.[115] Color changes were achieved via pH-dependent longitudinal grating period modulation by interweaving the pH-sensitive hydrogels with an IP-L photoresist. The dynamic structural color exhibited significant tunability, high sensitivity, and ultrafast recovery under incident light at 45 °. Additionally, a 4D printing-based grayscale design strategy enabled patterned encoding and array printing of dynamic structural colors, advancing applications in patterned printing, information encryption, and microfluidic chip sensing (Figure S2d).

5. CONCLUSION

Since its emergence in 2013, 4D printing has undergone rapid development and attracted significant attention across disciplines, owing to its versatility and broad applicability. With multidisciplinary collaboration, 4D printing is poised to address diverse challenges in a range of fields, and enhanced interdisciplinary integration may emerge as a key future direction.

The interplay of smart materials and 4D printing forms a mutually reinforcing cycle. Developments in 4D printing have driven innovations in smart materials, whose performance—including mechanical strength, response speed, and deformation accuracy—will continue to improve to meet increasingly complex demands. Future studies must focus on high-strength SMPs, rapid-response materials for near-instantaneous shape changes, and multifunctional materials that integrate sensing, actuation, self-healing, and self-diagnosis. Such materials enable 4D-printed objects to intelligently perceive and adapt to environmental stimuli, thereby advancing intelligent manufacturing.

The widespread adoption of 4D printing stems from its simplicity, structural flexibility, and compatibility with diverse materials. As a cross-disciplinary fabrication method, 4D printing customizes materials, printing techniques, and metastructures to meet the demands of specific applications, enabling the creation of innovative and intricate architectures across sectors, such as aerospace, biomedicine, and soft robotics. Future research must prioritize material development, printing precision enhancement, and interfacial bonding optimization. These advancements will propel intelligent manufacturing and accelerate industrial growth.

In summary, the unique capabilities of 4D printing in geometric morphing and functional reconfiguration demonstrate its significant potential in aerospace, healthcare, robotics, and electronics. However, most applications remain in nascent stages, constrained by challenges such as scalability and mass production. Progress in materials science, printing technologies, and cross-disciplinary integration will expand 4D printing applications and foster personalized production. With continued research and innovation, 4D printing promises transformative opportunities for innovation across industries.

■ ASSOCIATED CONTENT

Data Availability Statement

No data was used for the research described in the article.

Supporting Information

The Supporting Information is available free of charge at https://pubs.acs.org/doi/10.1021/acsapm.5c02816.

4D printing technologies and applications of 4D printing in other fields (PDF)

https://doi.org/10.1021/acsapm.5c02816
ACS Appl. Polym. Mater. 2025, 7, 14015−14032

AUTHOR INFORMATION

Corresponding Authors

Fenghua Zhang − *Centre for Composite Materials and Structures, Harbin Institute of Technology (HIT), Harbin 150080, People's Republic of China; Guangzhou Institute of Future Additive Manufacturing, Guangzhou 510150, People's Republic of China;* orcid.org/0000-0001-6136-9707; Email: fhzhang_hit@163.com

Linlin Wang − *Centre for Composite Materials and Structures, Harbin Institute of Technology (HIT), Harbin 150080, People's Republic of China; Guangzhou Institute of Future Additive Manufacturing, Guangzhou 510150, People's Republic of China*; Email: wangll_hit@163.com

Authors

Xixian Yu − *Centre for Composite Materials and Structures, Harbin Institute of Technology (HIT), Harbin 150080, People's Republic of China; Zhengzhou Research Institute, Harbin Institute of Technology (HIT), Zhengzhou 450000, People's Republic of China*

Jinsong Leng − *Centre for Composite Materials and Structures, Harbin Institute of Technology (HIT), Harbin 150080, People's Republic of China;* orcid.org/0000-0001-5098-9871

Complete contact information is available at: https://pubs.acs.org/10.1021/acsapm.5c02816

Notes

The authors declare no competing financial interest.

ACKNOWLEDGMENTS

This work is supported by the National Key R&D Program of China (2022YFB3805700), the National Natural Science Foundation of China (grant no. 92271112), and the China Postdoctoral Science Foundation (certificate no. 2024M764176).

REFERENCES

(1) Zou, S. Z.; Fan, S. N.; Oliveira, A. L.; Yao, X.; Zhang, Y. P.; Shao, H. L. 3D printed gelatin scaffold with improved shape fidelity and cytocompatibility by using silk fibroin nanofibers. *Adv. Fiber Mater.* **2022**, *4* (4), 758−773.

(2) Testoni, O.; Lumpe, T. S.; Huang, J.-L.; Wagner, M. A.; Bodkhe, S.; Zhakypov, Z.; Spolenak, R.; Paik, J. K.; Ermanni, P.; Muñoz, L.; et al. A 4D printed active compliant hinge for potential space applications using shape memory alloys and polymers. *Smart Mater. Struct.* **2021**, *30* (8), 085004.

(3) Mahmood, M. A. 3D printing in drug delivery and biomedical applications: A state-of-the-art review. *Compounds* **2021**, *1* (3), 94−115.

(4) Bao, C.; Moeinnia, H.; Kim, T.-H.; Lee, W.; Kim, W. S. 3D structural electronics via multi-directional robot 3D printing. *Adv. Mater. Technol.* **2023**, *8* (5), 2201349.

(5) Lazarus, N.; Tsang, H. H. 3-D printing structural electronics with conductive filaments. *IEEE Trans. Compon., Packag., Manuf. Technol.* **2020**, *10* (12), 1965−1972.

(6) Doshi, M.; Mahale, A.; Singh, S. K.; Deshmukh, S. Printing parameters and materials affecting mechanical properties of FDM-3D printed parts: perspective and prospects. *Mater. Today: Proc.* **2022**, *50*, 2269−2275.

(7) Kafle, A.; Luis, E.; Silwal, R.; Pan, H. M.; Shrestha, P. L.; Bastola, A. K. 3D/4D printing of polymers: Fused deposition modelling (FDM), selective laser sintering (SLS), and stereolithography (SLA). *Polymers* **2021**, *13* (18), 3101.

(8) Saadi, M. A. S. R.; Maguire, A.; Pottackal, N. T.; Thakur, M. S. H.; Ikram, M. M.; Hart, A. J.; Ajayan, P. M.; Rahman, M. M. Direct ink writing: A 3D printing technology for diverse materials. *Adv. Mater.* **2022**, *34* (28), 2108855.

(9) Valenzuela, C.; Ma, S.; Yang, Y.; Chen, Y.; Zhang, X.; Wang, L.; Feng, W. Direct ink writing of 3D chiral soft photonic crystals. *Adv. Funct. Mater.* **2025**, *35* (24), 2421280.

(10) Yang, L.; Liu, Y.; Bi, R.; Chen, Y.; Valenzuela, C.; Yang, Y.; Liu, H.; Wang, L.; Feng, W. Direct-Ink-Written shape-programmable micro-supercapacitors with electrothermal liquid crystal elastomers. *Adv. Funct. Mater.* **2025**, *35*, 2504979.

(11) Enayati-Gerdroodbar, A.; Khayati, A.; Ahmadi, M.; Pourabbas, B.; Aboudzadeh, M. A.; Salami-Kalajahi, M. An overview on potential of novel photoinitiators for vat photopolymerization-based 3D/4D printing formulations. *Eur. Polym. J.* **2024**, *221*, 113552.

(12) Nazir, A.; Gokcekaya, O.; Billah, K. M. M.; Ertugrul, O.; Jiang, J.; Sun, J.; Hussain, S. Multi-material additive manufacturing: A systematic review of design, properties, applications, challenges, and 3D printing of materials and cellular metamaterials. *Mater. Des.* **2023**, *226*, 111661.

(13) Tan, L. J.; Zhu, W.; Zhou, K. Recent progress on polymer materials for additive manufacturing. *Adv. Funct. Mater.* **2020**, *30* (43), 2003062.

(14) Gibson, I.; Rosen, D.; Stucker, B. *Additive manufacturing technologies 3D printing, rapid prototyping, and direct digital manufacturing*; Springer, 2015.

(15) Kuang, X.; Roach, D. J.; Wu, J.; Hamel, C. M.; Ding, Z.; Wang, T.; Dunn, M. L.; Qi, H. J. Advances in 4D printing: Materials and applications. *Adv. Funct. Mater.* **2019**, *29* (2), 1805290.

(16) Solórzano-Requejo, W.; Vega, C. A.; Martínez, R. Z.; Bodaghi, M.; Lantada, A. D. Ontology for smart 4D printed material systems and structures synergically applied with generative artificial intelligence for creativity promotion. *Smart Mater. Struct.* **2025**, *34* (1), 015045.

(17) Abdullah, T.; Okay, O. 4D printing of body temperature-responsive hydrogels based on poly(acrylic acid) with shape-memory and self-healing abilities. *ACS Appl. Bio Mater.* **2023**, *6* (2), 703−711.

(18) Fang, Z. Z.; Song, H. J.; Zhang, Y.; Jin, B. J.; Wu, J. J.; Zhao, Q.; Xie, T. Modular 4D printing via interfacial welding of digital light-controllable dynamic covalent polymer networks. *Matter* **2020**, *2* (5), 1187−1197.

(19) Chen, D. B.; Liu, Q. P.; Geng, P.; Tang, S. H.; Zhang, J. Q.; Wen, S. F.; Zhou, Y.; Yan, C. Z.; Han, Z. W.; Shi, Y. S. A 4D printing strategy and integrated design for programmable electroactive shape-color double-responsive bionic functions. *Compos. Sci. Technol.* **2021**, *208*, 108746.

(20) Lu, J.; Cui, H.; Xu, J.; Zhang, J.; Li, Z. 4D printing technology based on magnetic intelligent materials: Materials, processing processes, and application. *3D Print. Addit. Manuf.* **2024**, *11* (3), 1025−1041.

(21) Cremonini, A.; Sol, J. A. H. P.; Schenning, A. P. H. J.; Masiero, S.; Debije, M. G. The interplay between different stimuli in a 4D printed photo-, thermal-, and water-responsive liquid crystal elastomer actuator. *Chem.—Eur. J.* **2023**, *29* (36), No. e202300648.

(22) Zhang, F. H.; Wen, N.; Wang, L. L.; Bai, Y. Q.; Leng, J. S. Design of 4D printed shape-changing tracheal stent and remote controlling actuation. *Int. J. Smart Nano Mater.* **2021**, *12* (4), 375−389.

(23) Yan, S.; Zhang, F.; Luo, L.; Wang, L.; Liu, Y.; Leng, J. Shape memory polymer composites: 4D printing, smart structures, and applications. *Research* **2023**, *6*, 0234.

(24) Zhao, W.; Yue, C.; Liu, L.; Leng, J.; Liu, Y. Mechanical behavior analyses of 4D printed metamaterials structures with excellent energy absorption ability. *Compos. Struct.* **2023**, *304*, 116360.

(25) Wang, F.; Bi, R.; Chen, Y.; Yang, Y.; Liu, Y.; Yang, L.; Shen, Y.; Wang, L.; Feng, W. 4D printing of carbon-fiber-reinforced liquid crystal elastomers for self-deployable solar panels. *Mater. Horiz.* **2025**, *12* (14), 5315−5324.

(26) Vijay, K. M. G.; Kumar, S.; Doddamani, M. 4D printing of ultra-high performance shape memory polymer for space applications. *Adv. Eng. Mater.* **2024**, *26* (22), 2401427.
(27) Sun, J.; Du, L. Z.; Scarpa, F.; Liu, Y. J.; Leng, J. S. Morphing wingtip structure based on active inflatable honeycomb and shape memory polymer composite skin: A conceptual work. *Aerosp. Sci. Technol.* **2021**, *111*, 106541.
(28) Ni, C. J.; Chen, D.; Yin, Y.; Wen, X.; Chen, X. L.; Yang, C.; Chen, G. C.; Sun, Z.; Wen, J. H.; Jiao, Y. R.; et al. Shape memory polymer with programmable recovery onset. *Nature* **2023**, *622* (7984), 748−753.
(29) Deng, Y. D.; Yang, B. B.; Zhang, F. H.; Liu, Y. J.; Sun, J. B.; Zhang, S. Q.; Zhao, Y. T.; Yuan, H. P.; Leng, J. S. 4D printed orbital stent for the treatment of enophthalmic invagination. *Biomaterials* **2022**, *291*, 121886.
(30) Khalid, M. Y.; Arif, Z. U.; Noroozi, R.; Zolfagharian, A.; Bodaghi, M. 4D printing of shape memory polymer composites: A review on fabrication techniques, applications, and future perspectives. *J. Manuf. Processes* **2022**, *81*, 759−797.
(31) Kim, M. -S.; Heo, J. -K.; Rodrigue, H.; Lee, H. -T.; Pané, S.; Han, M. -W.; Ahn, S. -H. Shape memory alloy (SMA) actuators: The role of material, form, and scaling effects. *Adv. Mater.* **2023**, *35* (33), 2208517.
(32) Tabrizikahou, A.; Kuczma, M.; Łasecka-Plura, M.; Farsangi, E. N.; Noori, M.; Gardoni, P.; Li, S. Application and modelling of Shape-Memory Alloys for structural vibration control: State-of-the-art review. *Constr. Build. Mater.* **2022**, *342*, 127975.
(33) Wan, L.; Mao, Z.; Liu, H.; Xie, Y.; Lyu, F.; Cao, Z.; He, Y.; Yin, J.; Han, X.; Chan, W. Y. K.; et al. Direct 4D printing of gradient structure of ceramics. *Chem. Eng. J.* **2023**, *465*, 142804.
(34) Luo, L.; Zhang, F.; Leng, J. Shape memory epoxy resin and its composites: From materials to applications. *Research* **2022**, *2022*, 9767830.
(35) Wang, L.; Zhang, F.; Liu, Y.; Leng, J. Shape memory polymer fibers: Materials, structures, and applications. *Adv. Fiber Mater.* **2022**, *4* (1), 5−23.
(36) Li, Y.; Zhang, F.; Liu, Y.; Leng, J. A tailorable series of elastomeric-to-rigid, selfhealable, shape memory bismaleimide. *Small* **2023**, *20* (15), 2307244.
(37) Zhang, B.; Li, H.; Cheng, J.; Ye, H.; Sakhaei, A. H.; Yuan, C.; Rao, P.; Zhang, Y. -F.; Chen, Z.; Wang, R.; et al. Mechanically robust and UV-curable shape-memory polymers for digital light processing based 4D printing. *Adv. Mater.* **2021**, *33* (27), 2101298.
(38) Wang, J.; Lin, X.; Wang, R.; Lu, Y.; Zhang, L. Self-healing, photothermal-responsive, and shape memory polyurethanes for enhanced mechanical properties of 3D/4d printed objects. *Adv. Funct. Mater.* **2022**, *33* (15), 2211579.
(39) Luo, L.; Zhang, F.; Wang, L.; Liu, Y.; Leng, J. Recent advances in shape memory polymers: Multifunctional materials, multiscale structures, and applications. *Adv. Funct. Mater.* **2023**, *34* (14), 2312036.
(40) Bellin, I.; Kelch, S.; Langer, R.; Lendlein, A. Polymeric triple-shape materials. *Proc. Natl. Acad. Sci. U. S. A.* **2006**, *103* (48), 18043−18047.
(41) Xie, T. Tunable polymer multi-shape memory effect. *Nature* **2010**, *464* (7286), 267−270.
(42) Fang, Z. Z.; Lu, R. Z.; Chen, J. D.; Zhao, Q.; Wu, J. J. Vat photopolymerization of tough glassy polymers with multiple shape memory performances. *Addit. Manuf.* **2022**, *59*, 103171.
(43) Wang, L. L.; Zhang, F. H.; Du, S. Y.; Leng, J. S. 4D printing of triple-shape memory cyanate composites based on interpenetrating polymer network structures. *ACS Appl. Mater. Interfaces* **2023**, *15* (17), 21496−21506.
(44) Zare, M.; Prabhakaran, M. P.; Parvin, N.; Ramakrishna, S. Thermally-induced two-way shape memory polymers: Mechanisms, structures, and applications. *Chem. Eng. J.* **2019**, *374*, 706−720.
(45) Shi, Y. P.; Fang, G. Q.; Cao, Z. L.; Shi, F. Z.; Zhao, Q.; Fang, Z. Z.; Xie, T. Digital light fabrication of reversible shape memory polymers. *Chem. Eng. J.* **2021**, *426*, 131306.
(46) Guo, Y.; Chen, Y.; Yu, Q.; Liu, H.; Li, H.; Yu, Y. Ultra-tough and stress-free two-way shape memory polyurethane induced by polymer segment "spring". *Chem. Eng. J.* **2023**, *470*, 144212.
(47) Schenk, V.; Labastie, K.; Destarac, M.; Olivier, P.; Guerre, M. Vitrimer composites: current status and future challenges. *Mater. Adv.* **2022**, *3* (22), 8012−8029.
(48) Andreu, A.; Lee, H.; Kang, J.; Yoon, Y. -J. Self-healing materials for 3D printing. *Adv. Funct. Mater.* **2024**, *34* (30), 2315046.
(49) Jagadeesh, P.; Rangappa, S. M.; Siengchin, S.; Puttegowda, M.; Thiagamani, S. M. K.; Rajeshkumar, G.; Kumar, M. H.; Oladijo, O. P.; Fiore, V.; Cuadrado, M. M. M. Sustainable recycling technologies for thermoplastic polymers and their composites: A review of the state of the art. *Polym. Compos.* **2022**, *43* (9), 5831−5862.
(50) Ziaee, M.; Johnson, J. W.; Yourdkhani, M. 3D printing of short-carbon-fiber-reinforced thermoset polymer composites via frontal polymerization. *ACS Appl. Mater. Interfaces* **2022**, *14* (14), 16694−16702.
(51) Montarnal, D.; Capelot, M.; Tournilhac, F.; Leibler, L. Silica-like malleable materials from permanent organic networks. *Science* **2011**, *334* (6058), 965−968.
(52) Van Zee, N. J.; Nicolaÿ, R. Vitrimers: Permanently crosslinked polymers with dynamic network topology. *Prog. Polym. Sci.* **2020**, *104*, 101233.
(53) Utrera-Barrios, S.; Verdejo, R.; López-Manchado, M. A.; Santana, M. H. Evolution of self-healing elastomers, from extrinsic to combined intrinsic mechanisms: a review. *Mater. Horiz.* **2020**, *7* (11), 2882−2902.
(54) Pinho, A. C.; Buga, C. S.; Piedade, A. P. The chemistry behind 4D printing. *Appl. Mater. Today* **2020**, *19*, 100611.
(55) Wang, L.; Zhang, F.; Du, S.; Leng, J. 4D printing of shape-changing structures based on IPN epoxy composites formed by UV post-curing and γ-ray radiation. *Composites, Part A* **2022**, *162*, 107146.
(56) Feng, S. W.; Peng, X. L.; Cui, J. J.; Feng, R. Q.; Sun, Y. D.; Guo, Y. L.; Lu, Z.; Gao, W. Z.; Liu, F. K.; Liang, C.; et al. Photo switchable 4d printing remotely controlled responsive and mimetic deformation shape memory polymer nanocomposites. *Adv. Funct. Mater.* **2024**, *34* (28), 2401431.
(57) Chen, H. J.; Zhang, F. H.; Sun, Y.; Sun, B. Z.; Gu, B. H.; Leng, J. S.; Zhang, W. Electrothermal shape memory behavior and recovery force of four-dimensional printed continuous carbon fiber/polylactic acid composite. *Smart Mater. Struct.* **2021**, *30* (2), 025040.
(58) Dong, X. Y.; Zhang, F. H.; Wang, L. L.; Liu, Y. J.; Leng, J. S. 4D printing of electroactive shape-changing composite structures and their programmable behaviors. *Composites, Part A* **2022**, *157*, 106925.
(59) Zhang, F. H.; Zhang, Z. C.; Luo, C. J.; Lin, I. T.; Liu, Y. J.; Leng, J. S.; Smoukov, S. K. Remote, fast actuation of programmable multiple shape memory composites by magnetic fields. *J. Mater. Chem. C* **2015**, *3* (43), 11290−11293.
(60) Juan, L. T.; Lin, S. H.; Wong, C. W.; Jeng, U. S.; Huang, C. F.; Hsu, S. H. Functionalized cellulose nanofibers as crosslinkers to produce chitosan self-healing hydrogel and shape memory cryogel. *ACS Appl. Mater. Interfaces* **2022**, *14* (32), 36353−36365.
(61) Jin, F. K.; Wang, F. F.; Guo, P.; Lyu, M.; Wang, L. H.; Gao, D. L.; Sang, L. 4D printing of continuous carbon fiber reinforced composites with magneto-/electro-induced shape memory effect. *Chem. Eng. J.* **2025**, *508*, 160450.
(62) Li, H. J.; Bartolo, P. J. D.; Zhou, K. Direct 4D printing of hydrogels driven by structural topology. *Virtual Phys. Prototyping* **2025**, *20* (1), No. e2462962.
(63) Li, S.; Li, Z.; Mei, S.; Chen, X.; Ding, B.; Zhang, Y.; Zhao, W.; Zhang, X.; Cui, Z.; Fu, P.; et al. 4D printed thermoplastic polyamide elastomers with reversible two-way shape memory effect. *Adv. Mater. Technol.* **2023**, *8* (13), 2202066.
(64) Gu, F.; Ji, M.; Zhang, L.; Zhao, T.; Zhang, R.; Lv, X.; Tian, H.; Ma, X. Visualization of photocuring and 4D printing with real-time phosphorescence. *Nat. Commun.* **2025**, *16* (1), 4173.
(65) Zhou, Y. T.; Yang, Y. Z.; Jian, A. J.; Zhou, T. R.; Tao, G. M.; Ren, L. Q.; Zang, J. F.; Zhang, Z. H. Co-extrusion 4D printing of

shape memory polymers with continuous metallic fibers for selective deformation. *Compos. Sci. Technol.* **2022**, *227*, 109603.
(66) Wu, H. Z.; Wang, O. X.; Tian, Y. J.; Wang, M. Z.; Su, B.; Yan, C. Z.; Zhou, K.; Shi, Y. S. Selective laser sintering-based 4D printing of magnetism-responsive grippers. *ACS Appl. Mater. Interfaces* **2021**, *13* (11), 12679−12688.
(67) Wan, X.; Luo, L.; Liu, Y.; Leng, J. Direct ink writing based 4D printing of materials and their applications. *Adv. Sci.* **2020**, *7* (16), 2001000.
(68) Jiang, H.; Chung, C.; Dunn, M. L.; Yu, K. 4D printing of liquid crystal elastomer composites with continuous fiber reinforcement. *Nat. Commun.* **2024**, *15* (1), 8491.
(69) Huang, S.; Zhang, H.; Sheng, J.; Agyenim-Boateng, E.; Wang, C.; Yang, H.; Wei, J.; Jiang, G.; Zhou, J.; Lu, J. Digital light processing 4D printing multilayer polymers with tunable mechanical properties and shape memory behavior. *Chem. Eng. J.* **2023**, *465*, 142830.
(70) Zhou, T.; Zhang, L.; Yao, Q.; Ma, Y.; Hou, C.; Sun, B.; Shao, C.; Gao, P.; Chen, H. SLA 3D printing of high quality spine shaped β-TCP bioceramics for the hard tissue repair applications. *Ceram. Int.* **2020**, *46* (6), 7609−7614.
(71) Cui, C.; An, L.; Zhang, Z.; Ji, M.; Chen, K.; Yang, Y.; Su, Q.; Wang, F.; Cheng, Y.; Zhang, Y. Reconfigurable 4D printing of reprocessable and mechanically strong polythiourethane covalent adaptable networks. *Adv. Funct. Mater.* **2022**, *32* (29), 2203720.
(72) Romero-Ocaña, I.; Molina, S. I. Cork photocurable resin composite for stereolithography (SLA): Influence of cork particle size on mechanical and thermal properties. *Addit. Manuf.* **2022**, *51*, 102586.
(73) He, Y. J.; Wang, F.; Wang, X.; Zhang, J. N.; Wang, D. H.; Huang, X. B. A photocurable hybrid chitosan/acrylamide bioink for DLP based 3D bioprinting. *Mater. Des.* **2021**, *202*, 109588.
(74) He, C.; Ma, C.; Li, X. L.; Hou, F.; Yan, L. W.; Guo, A. R.; Liu, J. C. Continuous fast 3D printing of SiOC ceramic components. *Addit. Manuf.* **2021**, *46*, 102111.
(75) Pendry, J. B.; Schurig, D.; Smith, D. R. Controlling electromagnetic fields. *Science* **2006**, *312* (5781), 1780−1782.
(76) Xie, P. T.; Shi, Z. C.; Feng, M.; Sun, K.; Liu, Y.; Yan, K. L.; Liu, C. Z.; Moussa, T. A. A.; Huang, M. N.; Meng, S. W.; et al. Recent advances in radio-frequency negative dielectric metamaterials by designing heterogeneous composites. *Adv. Compos. Hybrid Mater.* **2022**, *5* (2), 679−695.
(77) Ren, X.; Das, R.; Tran, P.; Ngo, T. D.; Xie, Y. M. Auxetic metamaterials and structures: a review. *Smart Mater. Struct.* **2018**, *27* (2), 023001.
(78) Li, Y.; Chan, C. T.; Mazur, E. Dirac-like cone-based electromagnetic zero-index metamaterials. *Light: sci. Appl.* **2021**, *10* (1), 203.
(79) Xie, Y.; Ye, S.; Reyes, C.; Sithikong, P.; Popa, B. -I.; Wiley, B. J.; Cummer, S. A. Microwave metamaterials made by fused deposition 3D printing of a highly conductive copper-based filament. *Appl. Phys. Lett.* **2017**, *110* (18), 181903.
(80) Askari, M.; Hutchins, D. A.; Thomas, P. J.; Astolfi, L.; Watson, R. L.; Abdi, M.; Ricci, M.; Laureti, S.; Nie, L. Z.; Freear, S.; et al. Additive manufacturing of metamaterials: A review. *Addit. Manuf.* **2020**, *36*, 101562.
(81) Xin, X.; Yang, C.; Wang, Z.; Xing, Y.; Zeng, C.; Liu, L.; Liu, Y.; Leng, J. 4D printed mortise-tenon mechanical-electromagnetic multifunctional pixel metamaterials. *Chem. Eng. J.* **2025**, *504*, 158784.
(82) Yan, H.; Xie, S.; Zhang, F.; Jing, K.; He, L. Sound absorption performance of honeycomb metamaterials inspired by Mortise-and-Tenon structures. *Appl. Acoust.* **2025**, *228*, 110292.
(83) Huang, G.; Yengannagari, A. R.; Matsumori, K.; Patel, P.; Datla, A.; Trindade, K.; Amarsanaa, E.; Zhao, T.; Köhler, U.; Busko, D.; et al. Radiative cooling and indoor light management enabled by a transparent and self-cleaning polymer-based metamaterial. *Nat. Commun.* **2024**, *15* (1), 3798.
(84) Xin, X.; Liu, L.; Liu, Y.; Leng, J. 4D pixel mechanical metamaterials with programmable and reconfigurable properties. *Adv. Funct. Mater.* **2021**, *32* (6), 2107795.
(85) He, Q.; Zeng, Y.; Jiang, L.; Wang, Z.; Lu, G.; Kang, H.; Li, P.; Bethers, B.; Feng, S.; Sun, L.; et al. Growing recyclable and healable piezoelectric composites in 3D printed bioinspired structure for protective wearable sensor. *Nat. Commun.* **2023**, *14* (1), 6477.
(86) Xu, S. C.; Chen, N.; Qin, H. Y.; Zou, M.; Song, J. F. Biomimetic study of a honeycomb energy absorption structure based on straw micro-porous structure. *Biomimetics* **2024**, *9* (1), 60.
(87) Hang, G. G.; Liu, Z.; Fu, Y. X.; Cao, J. Y.; Wu, X. X.; Wang, X. C. Multidimensional bionic structure-based superhydrophobic and stretchable yarn sensor for motion monitoring. *ACS Appl. Nano Mater.* **2025**, *8* (5), 2432−2442.
(88) Deng, Y. D.; Zhang, F. H.; Liu, Y. J.; Zhang, S. Q.; Yuan, H. P.; Leng, J. S. 4D printed shape memory polyurethane-based composite for bionic cartilage scaffolds. *ACS Appl. Polym. Mater.* **2023**, *5* (2), 1283−1292.
(89) Lin, C.; Huang, Z.; Wang, Q.; Wang, W.; Wang, W.; Wang, Z.; Liu, L.; Liu, Y.; Leng, J. 3D printed bioinspired stents with photothermal effects for malignant colorectal obstruction. *Research* **2022**, *2022*, 9825656.
(90) Zhang, X. C.; Han, Y. S.; Zhu, M.; Chu, Y. H.; Li, W. D.; Zhang, Y. P.; Zhang, Y.; Luo, J. R.; Tao, R.; Qi, J. F. Bio-inspired 4D printed intelligent lattice metamaterials with tunable mechanical property. *Int. J. Mech Sci.* **2024**, *272*, 109198.
(91) Yan, S.; Liu, W. L.; Tan, X. J.; Meng, Z. Q.; Luo, W. J.; Jin, H.; Wen, Y. Z.; Sun, J. B.; Wu, L. L.; Zhou, J. Bio-inspired mechanical metamaterial with ultrahigh load-bearing capacity for energy dissipation. *Mater. Today* **2024**, *77*, 11−18.
(92) Zhang, D.; Liu, L.; Leng, J.; Liu, Y. Ultra-light release device integrated with screen-printed heaters for CubeSat's deployable solar arrays. *Compos. Struct.* **2020**, *232*, 111561.
(93) Xiao, H.; Wu, S.; Xie, D.; Guo, H.; Ma, L.; Wei, Y.; Liu, R. Shape memory polymer composite booms with applications in reel-type solar arrays. *Chin. J. Mech. Eng.* **2023**, *36* (1), 67.
(94) Lan, X.; Liu, L. W.; Pan, C. T.; Li, F. F.; Liu, Z. X.; Hou, G. H.; Sun, J.; Dai, W. X.; Wang, L. L.; Yue, H. H.; et al. Smart solar array consisting of shape-memory releasing mechanisms and deployable hinges. *AIAA J.* **2021**, *59* (6), 2200−2213.
(95) Zhou, Y. T.; Ren, L. Q.; Zang, J. F.; Zhang, Z. H. The shape memory properties and actuation performances of 4D printing poly (ether-ether-ketone). *Polymers* **2022**, *14* (18), 3800.
(96) Yang, P.; Ju, Y.; Hu, Y.; Xie, X.; Fang, B.; Lei, L. Emerging 3D bioprinting applications in plastic surgery. *Biomater. Res.* **2023**, *27* (1), s40824−022-00338-7.
(97) Wang, L.; Ma, J.; Guo, T.; Zhang, F.; Dong, A.; Zhang, S.; Liu, Y.; Yuan, H.; Leng, J. Control of surface wrinkles on shape memory PLA/PPDO micro-nanofibers and their applications in drug release and anti-scarring. *Adv. Fiber Mater.* **2023**, *5* (2), 632−649.
(98) Zhang, F. H.; Wang, L. L.; Zheng, Z. C.; Liu, Y. J.; Leng, J. S. Magnetic programming of 4D printed shape memory composite structures. *Composites, Part A* **2019**, *125*, 105571.
(99) Peng, W.; Yin, J.; Zhang, X.; Shi, Y.; Che, G.; Zhao, Q.; Liu, J. 4D printed shape memory anastomosis ring with controllable shape transformation and degradation. *Adv. Funct. Mater.* **2023**, *33* (20), 2214505.
(100) Qu, R. S.; Zhou, D.; Guo, T. T.; He, W. Y.; Cui, C. Q.; Zhou, Y. Y.; Zhang, Y. M.; Tang, Z. Z.; Zhang, X. R.; Wang, Q. H.; et al. 4D printing of shape memory inferior vena cava filters based on copolymer of poly(glycerol sebacate) acrylate-co-hydroxyethyl methacrylate (PGSA-HEMA). *Mater. Des.* **2023**, *225*, 111556.
(101) Zhang, C.; Cai, D. P.; Liao, P.; Su, J. W.; Deng, H.; Vardhanabhuti, B.; Ulery, B. D.; Chen, S. Y.; Lin, J. 4D Printing of shape-memory polymeric scaffolds for adaptive biomedical implantation. *Acta Biomater.* **2021**, *122*, 101−110.
(102) Zhai, F.; Feng, Y.; Li, Z.; Xie, Y.; Ge, J.; Wang, H.; Qiu, W.; Feng, W. 4D-printed untethered self-propelling soft robot with tactile perception: Rolling, racing, and exploring. *Matter* **2021**, *4* (10), 3313−3326.
(103) Gu, T.; Ji, T.; Bi, H.; Ding, K.; Sun, H.; Zhai, W.; Ren, Z.; Wei, Y.; Xu, M. 4D printed and multi-stimulus responsive shape

memory polymer nanocomposites developed on hydrogen bonding−metal-phenolic sacrificial network: Application for hazardous chemical operations soft robots. *Appl. Mater. Today* **2023**, *35*, 102009.
(104) Ferrer, J. M. M.; Cruz, R. E. S.; Caplan, S.; Van Rees, W. M.; Boley, J. W. Multiscale heterogeneous polymer composites for high stiffness 4D printed electrically controllable multifunctional structures. *Adv. Mater.* **2024**, *36* (30), 2405505.
(105) Zhang, L.; Huang, X.; Cole, T.; Lu, H.; Hang, J.; Li, W.; Tang, S.-Y.; Boyer, C.; Davis, T. P.; Qiao, R. 3D-printed liquid metal polymer composites as NIR-responsive 4D printing soft robot. *Nat. Commun.* **2023**, *14* (1), 7815.
(106) Deng, C. Y.; Qu, J. T.; Dong, J. H.; Guo, Y. F.; Wu, X. Z.; Fang, Y.; Sun, X. D.; Wei, Y. J.; Li, Z. K. 4D printing of magnetic smart structures based on light-cured magnetic hydrogel. *Chem. Eng. J.* **2024**, *494*, 152992.
(107) Ren, L.; Wang, Z. G.; Ren, L. Q.; Han, Z. W.; Zhou, X. L.; Song, Z. Y.; Liu, Q. P. 4D printing of shape-adaptive tactile sensor with tunable sensing characteristics. *Composites, Part B* **2023**, *265*, 110959.
(108) Ambulo, C. P.; Ford, M. J.; Searles, K.; Majidi, C.; Ware, T. H. 4D-printable liquid metal−liquid crystal elastomer composites. *ACS Appl. Mater. Interfaces* **2021**, *13* (11), 12805−12813.
(109) He, X. N.; Cheng, J. X.; Li, Z. Q.; Ye, H. T.; Wei, X. F.; Li, H. G.; Wang, R.; Zhang, Y. F.; Yang, H. Y.; Guo, C. F.; et al. Multimaterial three-dimensional printing of ultraviolet-curable ionic conductive elastomers with diverse polymers for multifunctional flexible electronics. *ACS Appl. Mater. Interfaces* **2023**, *15* (2), 3455−3466.
(110) Xing, R. Z.; Yang, J. Y.; Zhang, D. G.; Gong, W.; Neumann, T. V.; Wang, M. X.; Huang, R. L.; Kong, J.; Qi, W.; Dickey, M. D. Metallic gels for conductive 3D and 4D printing. *Matter* **2023**, *6* (7), 2248−2262.
(111) Zhang, S.; Xu, Y.; Li, Z.; Li, Y.; Lu, Z.; Chen, X.; Chen, P.; Chen, X.; Zhang, P.; Cai, C.; et al. Ultra-fast shape-deformation and highly-sensitive detection of 4D printed electromagnetic architectures. *Adv. Funct. Mater* **2024**, *34* (38), 2402563.
(112) Zhu, J. C.; Yang, Y. X.; Qiao, S. H.; Dai, H. J.; Chen, H.; Fu, Y.; Ma, L.; Wang, H. X.; Zhang, Y. H. 4D printing of betanin/gelatin/nano-chitin complexes-functionalized surimi via disulfide bonds, and its applicability in dysphagia diets. *Food Hydrocoll.* **2024**, *152*, 109891.
(113) Zhang, W.; Wang, H.; Wang, H.; Chan, J. Y. E.; Liu, H.; Zhang, B.; Zhang, Y. -F.; Agarwal, K.; Yang, X.; Ranganath, A. S.; et al. Structural multi-colour invisible inks with submicron 4D printing of shape memory polymers. *Nat. Commun.* **2021**, *12* (1), 112.
(114) Yang, Y.; Zhang, X.; Valenzuela, C.; Bi, R.; Chen, Y.; Liu, Y.; Zhang, C.; Li, W.; Wang, L.; Feng, W. High-throughput printing of customized structural-color graphics with circularly polarized reflection and mechanochromic response. *Matter* **2024**, *7* (6), 2091−2107.
(115) Wang, J.; Yu, H.; Zheng, J.; Zhang, Y.; Guo, H.; Qiu, Y.; Wang, X.; Yang, Y.; Liu, L. Nanograting-based dynamic structural colors using heterogeneous materials. *Nano-Micro Lett.* **2024**, *17* (1), 59.

https://doi.org/10.1021/acsapm.5c02816
ACS Appl. Polym. Mater. 2025, 7, 14015−14032